DISCUSSION

In our recent study using rats [24], after maternal exposure to MMI or PTU, we detected typical hypothyroidism-related changes in the thyroid-related hormone levels, and hippocampal CA1 pyramidal neurons due to neuronal mismigration, as previously reported [8]. We also observed white matter changes, which seem to be due to impaired oligodendroglial development [6, 21]. To visualize molecules related to impaired neuronal development, microdissected CA1 region-specific global gene expression profiling was performed in the present study using the same animals that were used in our previous study. Two recently published studies have used microarrays to examine the expression profiles in the cerebral cortex and hippocampus of genes linked to developmental hypothyroidism caused by maternal PTU-exposure [7, 19]. In accordance with these studies, the genes that were significantly down-regulated in the present study included those that play roles in myelination, such as *Mobp* and myelin-associated glycoprotein, suggestive of the reflection of suppressed myelination by developmental hypothyroidism [21]. However, the genes that were found to be up-regulated on microdissected CA1 pyramidal cell layer, including *Efna5* and *Tacr3*, in the present study, have not been identified in previous studies. This difference may be related to the target tissues collected and the methods used, including microdissection of CA1 pyramidal cell layer from paraffin-embedded sections in the present study versus manual dissection of the cortical tissues from unfixed tissues in the previous studies.

EphA5 is a tyrosine kinase receptor that is almost exclusively expressed in the nervous system [15]. EphA5 and its ligand are important in mediating axon guidance, topographic projection, development, cell migration and the plasticity of limbic structures [15]. In addition, the transient expression of EphA5 during development is correlated with early neurogenesis and the migration of differentiated cells in the midbrain [3]. Thus, although expression of EphA5 was mostly weak in the euthyroid CA1 pyramidal neurons at PND 20, the increased number of EphA5-expressing cells with strong intensity in the CA1 region during developmental hypothyroidism in the present study reflects the neuronal mismigration caused by anti-thyroid agents. However, this increase was recovered after cessation of developmental hypothyroidism. Ephrins and their receptors are recently identified molecules and functional relationship between subfamily proteins is largely unknown; however, we, in the present study, found down-regulation of Epha7, another subfamily ephrin receptor, in all exposure groups of anti-thyroid agents (Table 1).

Tacr3, a member of the mammalian tachykinin peptide neurotransmitter/neuromodulator receptor family, is predominantly expressed in neurons in both the peripheral and central nervous systems, including the hippocampus [25]. There is increasing evidence of the role of Tacr3 on the survival and function of dopaminergic neurons. The survival of mesencephalic dopaminergic neurons during development largely depends on excitatory inputs, and tachykinins, through their receptors, are reported to play role in excitation [20]. On the other hand, senktide, a Tacr3 agonist, activates dopaminergic neurons to stimulate the release of dopamine and serotonin, and hyperlocomotion in gerbils [14]. Abnormal excitatory action of D_2-like receptor, one of the major subtypes of dopaminergic receptors, was observed on glutamatergic transmission in the CA1 synapses in the adult stage of rats after developmental hypothyroidism, suggesting a permanent disruption of synaptic integration in the CA1 neural networks [16]. While the role of Tacr3 in the hippocampal CA1 region during development is not clear, the increase in Tacr3-positive cells with strong intensity in this region during developmental hypothyroidism suggests a cell survival effect of tachykinin-3. Although the magnitude of the change was decreased, as compared with that at the end of the developmental hypothyroidism, the increased number of Tacr3-positive cells in the CA1 region of MMI and 3 ppm PTU-exposed animals may be an outcome of permanent disruption of synaptic integration, as described by Oh-Nishi *et al.* [16]. However, sparse distribution of Tacr3-positive cells may reflect that impairment sustained in a small population of aberrantly migrated neurons.

In conclusion, in this study, we have shown gene expression profiles showing altered expression in response to developmental hypothyroidism by analysis on microdissected hippocampal CA1 pyramidal cell layer in rats. Immunohistochemical analysis of the two candidate molecules revealed that developmental hypothyroidism until weaning is associated with the persistence of Tacr3-expressing neurons until the adult stage in the CA1 region, suggestive of the reflection of permanent disruption of synaptic integration. These findings probably reflect a mechanism to facilitate cell survival of aberrantly developed neurons due to mismigration.

ACKNOWLEDGMENT(S). We thank Miss Tomomi Morikawa for her technical assistance in conducting the animal study. We also thank Mrs. Shigeko Suzuki and Miss Ayako Kaneko for their technical assistance in preparing the histological specimens. This work was supported in part by Health and Labour Sciences Research Grants (Research on Risk of Chemical Substances) from the Ministry of Health, Labour and Welfare of Japan. All of the authors disclose that there are no conflicts of interest that could inappropriately influence the outcomes of the present study.

REFERENCES

1. Akaike, M., Kato, N., Ohno, H. and Kobayashi, T. 1991. Hyperactivity and spatial maze learning impairment of adult rats with temporary neonatal hypothyroidism. *Neurotoxicol. Teratol.* **13**: 317–322.
2. Comer, C. P. and Norton, S. 1982. Effects of perinatal methimazole exposure on a developmental test battery for neurobehavioral toxicity in rats. *Toxicol. Appl. Pharmacol.* **63**: 133–141.
3. Cooper, M. A., Crockett, D. P., Nowakowski, R. S., Gale, N. W. and Zhou, R. 2009. Distribution of EphA5 receptor protein

in the developing and adult mouse nervous system. *J. Comp. Neurol.* **514**: 310–328.
4. de Escobar, G. M., Obregón, M. J. and del Rey, F. E. 2007. Iodine deficiency and brain development in the first half of pregnancy. *Public Health Nutr.* **10**: 1554–1570.
5. Gerlai, R., Shinsky, N., Shih, A., Williams, P., Winer, J., Armanini, M., Cairns, B., Winslow, J., Gao, W. and Phillips, H. S. 1999. Regulation of learning by EphA receptors: a protein targeting study. *J. Neurosci.* **19**: 9538–9549.
6. Goodman, J. H. and Gilbert, M. E. 2007. Modest thyroid hormone insufficiency during development induces a cellular malformation in the corpus callosum: a model of cortical dysplasia. *Endocrinology* **148**: 2593–2597.
7. Kobayashi, K., Akune, H., Sumida, K., Saito, K., Yoshioka, T. and Tsuji, R. 2009. Perinatal exposure to PTU decreases expression of Arc, Homer 1, Egr 1 and Kcna 1 in the rat cerebral cortex and hippocampus. *Brain Res.* **1264**: 24–32.
8. Lavado-Autric, R., Ausó, E., García-Velasco, J. V., Arufe Mdel, C., Escobar del Rey, F., Berbel, P. and Morreale de Escobar, G. 2003. Early maternal hypothyroxinemia alters histogenesis and cerebral cortex cytoarchitecture of the progeny. *J. Clin. Invest.* **111**: 954–957.
9. Lee, K-Y., Shibutani, M., Inoue, K., Kuroiwa, K., U, M., Woo, G-H. and Hirose, M. 2006. Methacarn fixation—Effects of tissue processing and storage conditions on detection of mRNAs and proteins in paraffin-embedded tissues. *Anal. Biochem.* **351**: 36–43.
10. Masutomi, N., Shibutani, M., Takagi, H., Uneyama, C., Takahashi, N. and Hirose, M. 2003. Impact of dietary exposure to methoxychlor, genistein, or diisononyl phthalate during the perinatal period on the development of the rat endocrine/reproductive systems in later life. *Toxicology* **192**: 149–170.
11. Mileusnic, D., Lee, J. M., Magnuson, D. J., Hejna, M. J., Krause, J. E., Lorens, J. B. and Lorens, S. A. 1999. Neurokinin-3 receptor distribution in rat and human brain: an immunohistochemical study. *Neuroscience* **89**: 1269–1290.
12. Montero-Pedrazuela, A., Venero, C., Lavado-Autric, R., Fernández-Lamo, I., García-Verdugo, J. M., Bernal, J. and Guadaño-Ferraz, A. 2006. Modulation of adult hippocampal neurogenesis by thyroid hormones: implications in depressive-like behavior. *Mol. Psychiatry* **11**: 361–371.
13. Nakamura, R., Teshima, R., Hachisuka, A., Sato, Y., Takagi, K., Nakamura, R., Woo, G-H., Shibutani, M. and Sawada, J. 2007. Effects of developmental hypothyroidism induced by maternal administration of methimazole or propylthiouracil on the immune system of rats. *Int. Immunopharmacol.* **7**: 1630–1638.
14. Nordquist, R. E., Durkin, S., Jacquet, A. and Spooren, W. 2008. The tachykinin NK3 receptor agonist senktide induces locomotor activity in male Mongolian gerbils. *Eur. J. Pharmacol.* **600**: 87–92.
15. Numachi, Y., Yoshida, S., Yamashita, M., Fujiyama, K., Toda, S., Matsuoka, H., Kajii, Y. and Nishikawa, T. 2007. Altered EphA5 mRNA expression in rat brain with a single methamphetamine treatment. *Neurosci. Lett.* **424**: 116–121.
16 Oh-Nishi, A., Saji, M., Furudate, S. I. and Suzuki, N. 2005. Dopamine D_2-like receptor function is converted from excitatory to inhibitory by thyroxine in the developmental hippocampus. *J. Neuroendocrinol.* **17**: 836–845.
17. Olivieri, G. and Miescher, G. C. 1999. Immunohistochemical localization of EphA5 in the adult human central nervous system. *J. Histochem. Cytochem.* **47**: 855–861.
18. Porterfield, S. P. 2000. Thyroidal dysfunction and environmental chemicals—Potential impact on brain development. *Environ. Health Perspect.* **108**: 433–438.
19. Royland, J. E., Parker, J. S. and Gilbert, M. E. 2008. A genomic analysis of subclinical hypothyroidism in hippocampus and neocortex of the developing rat brain. *J. Neuroendocrinol.* **20**: 1319–1338.
20. Salthun-Lassalle, B., Traver, S., Hirsch, E. C. and Michel, P. P. 2005. Substance P, neurokinins A and B, and synthetic tachykinin peptides protect mesencephalic dopaminergic neurons in culture via an activity-dependent mechanism. *Mol. Pharmacol.* **68**: 1214–1224.
21. Schoonover, C. M., Seibel, M. M., Jolson, D. M., Stack, M. J., Rahman, R. J., Jones, S. A., Mariash, C. N. and Anderson, G. W. 2004 Thyroid hormone regulates oligodendrocyte accumulation in developing rat brain white matter tracts. *Endocrinology* **145**: 5013–5020.
22. Shibutani, M., Uneyama, C., Miyazaki, K., Toyoda, K. and Hirose, M. 2000. Methacarn fixation: a novel tool for analysis of gene expressions in paraffin-embedded tissue specimens. *Lab. Invest.* **80**: 199–208.
23. Shibutani, M., Lee, K-Y., Igarashi, K., Woo, G-H., Inoue, K., Nishimura, T. and Hirose, M. 2007. Hypothalamus region-specific global gene expression profiling in early stages of central endocrine disruption in rat neonates injected with estradiol benzoate or flutamide. *Dev. Neurobiol.* **67**: 253–269.
24. Shibutani, M., Woo, G-H., Fujimoto, H., Saegusa, Y., Takahashi, M., Inoue, K., Hirose, M. and Nishikawa, A. 2009. Assessment of developmental effects of hypothyroidism in rats from in utero and lactation exposure to anti-thyroid agents. *Reprod. Toxicol.* **28**: 297–307.
25. Smith, P. W. and Dawson, L. A. 2008. Neurokinin 3 (NK3) receptor modulators for the treatment of psychiatric disorders. *Recent Pat. CNS Drug Discov.* **3**: 1–15.
26. Takagi, H., Shibutani, M., Kato, N., Fujita, H., Lee, K-Y., Takigami, S., Mitsumori, K. and Hirose, M. 2004. Microdissected region-specific gene expression analysis with methacarn-fixed, paraffin-embedded tissues by real-time RT-PCR. *J. Histochem. Cytochem.* **52**: 903–913.
27. Uneyama, C., Shibutani, M., Masutomi, N., Takagi, H. and Hirose, M. 2002. Methacarn fixation for genomic DNA analysis in microdissected, paraffin-embedded tissue specimens. *J. Histochem. Cytochem.* **50**: 1237–1245.
28. Woo, G-H., Takahashi, M., Inoue, K., Fujimoto, H., Igarashi, K., Kanno, J., Hirose, M., Nishikawa, A. and Shibutani, M. 2009. Cellular distributions of molecules with altered expression specific to thyroid proliferative lesions developing in a rat thyroid carcinogenesis model. *Cancer Sci.* **100**: 617–625.

Reproductive Toxicology 29 (2010) 407–414

Contents lists available at ScienceDirect

Reproductive Toxicology

journal homepage: www.elsevier.com/locate/reprotox

Sustained production of Reelin-expressing interneurons in the hippocampal dentate hilus after developmental exposure to anti-thyroid agents in rats

Yukie Saegusa[a,b], Gye-Hyeong Woo[c], Hitoshi Fujimoto[c], Sayaka Kemmochi[a,b], Keisuke Shimamoto[a,b], Masao Hirose[c,d], Kunitoshi Mitsumori[a], Akiyoshi Nishikawa[c], Makoto Shibutani[a,c,*]

[a] Laboratory of Veterinary Pathology, Tokyo University of Agriculture and Technology, 3-5-8 Saiwai-cho, Fuchu-shi, Tokyo 183-8509, Japan
[b] Pathogenetic Veterinary Science, United Graduate School of Veterinary Sciences, Gifu University, 1-1 Yanagido, Gifu-shi, Gifu 501-1193, Japan
[c] Division of Pathology, National Institute of Health Sciences, 1-18-1 Kamiyoga, Setagaya-ku, Tokyo 158-8501, Japan
[d] Food Safety Commission, Akasaka Park Bld. 22nd F. 5-2-20 Akasaka, Minato-ku, Tokyo 100-8989, Japan

ARTICLE INFO

Article history:
Received 16 November 2009
Received in revised form 23 February 2010
Accepted 21 March 2010
Available online 27 March 2010

Keywords:
Developmental hypothyroidism
Impaired brain development
Migration
Neurogenesis
Dentate gyrus
Reelin
GABAergic interneuron

ABSTRACT

To detect molecular evidence reflecting a permanent disruption of neuronal development due to hypothyroidism, distribution of Reelin-producing cells that function in neuronal migration and positioning was analyzed in the hippocampal dentate hilus using rats. From gestation day 10, maternal rats were administered either 6-propyl-2-thiouracil (PTU) at 3 or 12 ppm (0.57 or 1.97 mg/kg body weight/day) or methimazole (MMI) at 200 ppm (27.2 mg/kg body weight/day) in the drinking water and male offspring were immunohistochemically examined at the end of exposure on weaning (postnatal day 20) and at the adult stage (11-week-old). Offspring with MMI and 12 ppm PTU displayed evidence of growth retardation lasting into the adult stage. On the other hand, all exposure groups showed a sustained increase in Reelin-expressing cells in the dentate hilus until the adult stage in parallel with Calbindin-D-28K-expressing cells at weaning and with glutamic acid decarboxylase 67-positive cells in the adult stage, confirming an increase in γ-aminobutyric acid (GABA)ergic interneurons. At the adult stage, NeuN-positive postmitotic mature neurons were also increased in the hilus in all exposure groups, however, the increased population of Reelin-producing cells at this stage was either weakly positive or negative for NeuN, indicative of immature neurons. At weaning, neuroblast-producing subgranular zone of the dentate gyrus showed increased apoptosis and decreased cell proliferation suggestive of impaired neurogenesis. The results suggest that sustained increases of immature GABAergic interneurons synthesizing Reelin in the hilus could be a signature of compensatory regulation for impaired neurogenesis and mismigration during the neuronal development as a hypothyroidism-related brain effect rather than that secondary to systemic growth retardation.

1. Introduction

Thyroid hormones are essential for normal fetal and neonatal brain development. They control neuronal and glial proliferation in definitive brain regions and regulate neural migration and differentiation [1–3]. In humans, maternal hypothyroxinemia, early in pregnancy, may have adverse effects on fetal brain development and importantly, even mild–moderate hypothyroxinemia may result in suboptimal neurodevelopment [4]. These results may increase the concern of impaired brain development by exposure to thyroid hormone-disrupting chemicals in the environment. Particularly, groups of persistent organic pollutants, such as organochlorine pesticides and polychlorinated biphenyls, have been shown to be ubiquitous environmental pollutants because of their great chemical stability and lipid solubility [5]. In addition to the variety of effects including immunologic, teratogenic, reproductive, carcinogenic, and neurological effects [6], many of these compounds are known to induce hypothyroidism [7].

Experimentally, developmental hypothyroidism leads to growth retardation, neurological defects and impaired performance on a variety of behavioral learning actions [8,9]. Rat offspring exposed maternally to anti-thyroid agents such as 6-propyl-2-thiouracil (PTU) show impaired brain development, with impaired neuronal migration and white matter hypoplasia involving limited axonal myelination and oligodendrocytic

Abbreviations: CA1, cornu ammonis 1; CA2, cornu ammonis 2; CA3, cornu ammonis 3; Calb-D-28K, Calbindin-D-28K; DH, dentate hilus; GABA, γ-aminobutyric acid; GAD67, glutamic acid decarboxylase 67; GD, gestation day; MMI, methimazole; NeuN, neuron-specific nuclear protein; PCNA, proliferating cell nuclear antigen; PND, postnatal day; PNW, postnatal week; PTU, 6-propyl-2-thiouracil; T_3, triiodothyronine; T_4, thyroxine; TSH, thyroid-stimulating hormone.

* Corresponding author at: Laboratory of Veterinary Pathology, Tokyo University of Agriculture and Technology, 3-5-8 Saiwai-cho, Fuchu-shi, Tokyo 183-8509, Japan. Tel.: +81 42 367 5874; fax: +81 42 367 5771.
E-mail address: mshibuta@cc.tuat.ac.jp (M. Shibutani).

0890-6238/$ – see front matter © 2010 Elsevier Inc. All rights reserved.
doi:10.1016/j.reprotox.2010.03.006

Table 1
Serum levels of thyroid-related hormones of the male offspring exposed to anti-thyroid agents during the period from the mid-gestation and lactation periods.

		Anti-thyroid agent in the drinking water		
	Untreated controls	200 ppm MMI	3 ppm PTU	12 ppm PTU
PND 20				
No. of offspring examined	10	9	10	9[a]
T_3 (ng/ml)	1.22 ± 0.10[b]	0.43 ± 0.19**	0.97 ± 0.31*	0.25 ± 0.03**
T_4 (μg/ml)	4.72 ± 0.84	1.06 ± 0.44**	1.86 ± 0.41**	1.06 ± 0.32**
TSH (ng/ml)	6.80 ± 2.11	35.33 ± 12.69**	27.38 ± 13.66**	27.69 ± 5.74**
PNW 11				
No. of offspring examined	10	10	10	6
T_3 (ng/ml)	1.02 ± 0.08	0.88 ± 0.09**	0.93 ± 0.11	0.84 ± 0.10**
T_4 (μg/ml)	5.11 ± 0.70	4.57 ± 1.04	5.12 ± 0.73	4.05 ± 0.71
TSH (ng/ml)	9.81 ± 3.16	9.41 ± 4.40	9.10 ± 3.25	7.75 ± 2.23

[a] $N = 7$ for measurement of T_3 and T_4 levels.
[b] Mean ± SD.
* Significantly different from the untreated controls ($^*P < 0.05$).
** Significantly different from the untreated controls ($^{**}P < 0.01$).

accumulation [2,10,11]. The outcome of this type of impaired brain development is permanent and is accompanied by apparent structural and functional abnormalities. However, it is still unclear whether the molecular aberrations remain in the retarded brain after maturation.

In the hippocampal formation, neuronal subpopulations are known to produce Reelin from embryonic period throughout adult life [12–16]. Reelin is a secreted extracellular matrix glycoprotein that plays a critical role in neuronal migration and positioning during brain development in the process regulated by thyroid hormone [13,17]. Also, in adults, it is suggested that Reelin released by γ-aminobutyric acid (GABA)ergic interneurons could regulate the migration and maturation of newborn granular cells in the dentate granular cell layer [18]. Altered Reelin signaling has been reported in the dentate gyrus of some neurological disease conditions, such as depression and epilepsy [18,19]. Within hippocampal formation, dentate gyrus is the unique structure that can continue neurogenesis during postnatal life and is a well-known target of developmental hypothyroidism [20].

In the present study, to detect a key molecular event reflecting permanent disruption of neuronal development due to exposure to xenobiotic chemicals that can interfere with thyroid hormone signaling, we examined temporal distribution change of Reelin-expressing cells in the dentate gyrus of rat offspring after developmental exposure to anti-thyroid agents. To distinguish chemical-specific expression changes from hypothyroidism-linked ones, two different anti-thyroid agents, methimazole (MMI) and PTU, were used, and dose-related responses were also examined with PTU.

Because of the similarities in the DNA binding domain of estrogen response element and thyroid hormone response element, crosstalk between the estrogen receptors and thyroid hormone receptors has been reported in previous studies [21,22]. Therefore, male offspring were selected for immunohistochemical analysis as well as measurement of serum thyroid-related hormones to avoid possible influence of estrogen in the present study.

2. Materials and methods

2.1. Chemicals and animals

Methimazole (2-mercapto-1-methylimidazole: MMI; CAS No. 60-56-0) and 6-propyl-2-thiouracil (PTU; CAS No. 51-52-5) were obtained from Sigma Chemical Co. (St. Louis, MO, USA). Pregnant Crj:CD®(SD)IGS rats were purchased from Charles River Japan Inc. (Yokohama, Japan) at gestation day (GD) 3 (appearance of vaginal plugs was designated as GD 0). Animals were housed individually in polycarbonate cages with wood chip bedding, maintained in an air-conditioned animal room (temperature: 24 ± 1 °C; relative humidity: 55 ± 5%) with a 12-h light/dark cycle and allowed *ad libitum* access to food and tap water. A soy-free diet (Oriental Yeast Co. Ltd., Tokyo, Japan) was chosen as the basal diet for the maternal animals to eliminate possible phytoestrogen effects [23], and water was given *ad libitum* throughout the experimental period including the 1-week acclimation period. On the other hand, all offspring consumed a regular CRF-1 basal diet (Oriental Yeast Co. Ltd.) and water *ad libitum* from PND 20 onwards (PND 0: the day of delivery). Although the formula is not open, CRF-1 contains soybean/alfalfa-derived proteins and oil including daidzin and genistin at concentrations of 87 and 102 ppm in diet according to the supplier's analysis, and coumestrol of less than 3 ppm based on the content of lucerne meal in the diet (supplier's comment). Soy-free diet was prepared based on the formulation of the NIH-07 open formula rodent diet, in which soybean meal and soy oil were replaced with ground corn, ground wheat, wheat middlings and corn oil. Values for phytoestrogens in this diet were below the detection limit (0.5 ppm), except for coumestrol with 3 ppm. Estrogen equivalents of phytoestrogens included in each CRF-1 and soy-free diet were roughly calculated as 0.91 and 0.06 ppm of β-estradiol, respectively, based on the relative binding affinities in a rat endometrial-derived experimental model [24]. Nutritional standards did not differ between soy-free diet and CRF-1 (supplier's analysis).

2.2. Experimental design

The animal experiments were identical to those in a previous study [25]. In brief, maternal animals were randomly divided into four groups including untreated controls. Eight dams per group were treated with 200 ppm of MMI or 3 ppm or 12 ppm of PTU in the drinking water from GD 10 to PND 20. Dose finding study on PTU and MMI was preliminarily performed based on the dose range to show changes in neuronal or oligodendroglial parameters in previous reports [2,26–28]. With the dose setting at the level of 9 ppm or 12 ppm for PTU and 200 ppm or 250 ppm for MMI in the drinking water, dams ($n = 2$/dose) were treated from GD 10 to PND 20, apart from the untreated control dams ($n = 2$). As a result, PTU at 12 ppm and MMI at 200 ppm exhibited clear hypothyroidism-linked effects to dams, i.e., increased relative thyroid weights and thyroid follicular cell hypertrophy, but did not affect pregnancy, implantation, delivery, or nursing until PND 20 (data not shown).

On PND 2, the litters were culled randomly, leaving four male and four female offspring. On PND 20, 20 male and 20 female offspring (at least one male and one female per dam) per group were subjected to prepubertal necropsy [25,29].

The remaining animals were maintained until postnatal week (PNW) 11. All offspring consumed the CRF-1 basal diet and tap water *ad libitum* from PND 20 onwards. At PNW 11, all pups were subjected to adult stage necropsy [25,29].

All animals used in the present study were weighed and sacrificed by exsanguination from the abdominal aorta under deep anesthesia with ether. These protocols were reviewed in terms of animal welfare and approved by the Animal Care and Use Committee of the National Institute of Health Sciences, Japan.

2.3. Thyroid-related hormone measurement

At the necropsies of animals sacrificed on PND 20 and PNW 11, blood samples of male offspring were collected from the abdominal aorta under anesthesia. Serum was prepared and stored at −30 °C to measure thyroid-stimulating hormone (TSH), triiodothyronine (T_3) and thyroxine (T_4) concentrations at SRL, Inc. (Tokyo, Japan). Number of animals examined was described in Table 1.

2.4. Immunohistochemistry and Cresyl Violet staining

To evaluate the immunohistochemical distribution of the molecules, brains in the subgroups of male offspring killed at PND 20 and PNW 11 were fixed in Bouin's solution at room temperature overnight. Six animals were used as untreated controls, six for 200 ppm MMI, eight for 3 ppm PTU, and nine for 12 ppm PTU on PND 20.

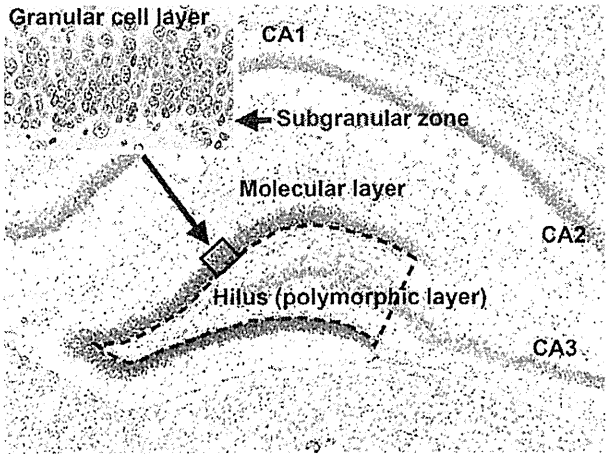

Fig. 1. Overview of the hippocampal formation of a male rat at postnatal day 20 stained with hematoxylin and eosin. Inset shows higher magnification of the granular cell layer and subgranular zone. Magnification, 40× (Inset: 200×). Number of immunoreactive cells for Reelin, Calb-D-28K, and GAD67 in the hilus of the dentate gyrus, as enclosed by the dotted line, was counted and normalized for the unit area. Small-sized neurons in this area showed positive immunoreactivity with these antigens, but large-sized CA3 neurons distributed in this area were not immunoreactive with these antigens. Number of NeuN-immunoreactive cells was similarly counted and normalized for the unit area, but CA3 neurons distributed in this area and also positive for NeuN were excluded from counting.

On PNW 11, 10 animals were used as untreated controls and 10 for 200 ppm MMI, nine for 3 ppm PTU, and six for 12 ppm PTU. Coronal slices at the positions of −3.0 and −3.5 mm from the bregma were prepared from brains of PND 20 and PNW 11, respectively.

Immunohistochemistry was performed on the brain sections (3 μm in thickness) of PND 20 and PNW 11 animals with antibodies against Reelin (clone G10, mouse $IgG_{1\kappa}$, 1:1000; Novus Biologicals, Inc., Littleton, CO, USA) and Calbindin-D-28K (Calb-D-28K; clone CB-955, mouse IgG_1, 1:500; Sigma Chemical Co.), which were incubated with the tissue sections overnight at 4 °C. On the brain sections at PNW 11, immunohistochemistry of neuron-specific nuclear protein (NeuN; clone A60, mouse IgG_1, 1:1000, Chemicon, Billerica, MA, USA), which specifically detects postmitotic neurons, was also performed. In addition, immunohistochemistry of glutamic acid decarboxylase 67 (GAD67; clone 1G10.2, mouse IgG, 1:50, Chemicon) and proliferating cell nuclear antigen (PCNA; clone PC10, mouse IgG_{2a}, 1:200, Dako, Glostrup, Denmark) was performed on PND 20 and PNW 11 ($n=5$ in each group) in untreated controls and rats treated with 12 ppm PTU. Antigen retrieval treatment was not performed for these antigens. Immunodetection was carried out using a VECTASTAIN® Elite ABC kit (Vector Laboratories Inc., Burlingame, CA, USA) with 3,3′-diaminobenzidine/H_2O_2 as the chromogen, as previously described [30]. The sections were then counterstained with hematoxylin and coverslipped for microscopic examination.

For double staining of NeuN and Reelin, 3,3′,5,5′-tetramethylbenzidine (Vector Laboratories) was used to visualize Reelin and DAB was used to visualize NeuN.

For evaluation of apoptosis in the subgranular zone of the dentate gyrus, apoptotic bodies were detected by Cresyl Violet staining as described by others [31].

2.5. Morphometry of immunolocalized cells and apoptotic cells

Reelin-, NeuN-, Calb-D-28K- or GAD67-positive cells distributed in the hilus of the dentate gyrus were bilaterally counted and normalized for the number per unit area of the hilar area (polymorphic layer) as enclosed by the dotted line in Fig. 1. In the subgranular zone of the dentate gyrus (Inset of Fig. 1), apoptotic bodies as detected by Cresyl Violet staining and proliferating cells as detected by nuclear immunoreactivity of PCNA were bilaterally counted and normalized the number with the length of the granular cell layer measured. For quantitative measurement of each immunoreactive cellular component, digital photomicrographs at 100-fold magnification were taken using a BX51 microscope (Olympus Optical Co., Ltd., Tokyo, Japan) attached to a DP70 Digital Camera System (Olympus Optical Co.), and quantitative measurements were performed using the WinROOF image analysis software package (version 5.7, Mitani Corp., Fukui, Japan).

2.6. Statistical analysis

Numerical data of the thyroid-related hormone levels and the number of immunoreactive cells were assessed using Student's *t*-test to compare the untreated controls with each of the anti-thyroid agent-exposed groups when the variance was homogenous among the groups using a test for equal variance. If a significant difference in variance was observed, Aspin–Welch's *t*-test was used instead.

3. Results

3.1. Effects on dams

During the gestation period, slight but statistically significant decrease of water consumption during GD 10–GD 15 and food intake during GD 15–GD 20 were observed with 200 ppm MMI compared with the untreated dams [25]. During the lactation period, both water consumption and food intake of dams decreased with 12 ppm PTU and MMI with statistical significance. However, treatment did not affect the body weight gain during the exposure period and the body weight of dams at weaning [25]. With regard to the maternal clinical signs, all dams in the groups of 12 ppm PTU and MMI exhibited somewhat higher sensitivity against handling stimuli as compared with untreated controls and 3 ppm PTU after delivery. However, no dams abandoned rearing offspring.

By monitoring water consumption, chemical intake of dams treated with 3 ppm PTU was calculated to be 0.57 mg/kg body weight/day during the whole exposure period (0.39 mg/kg body weight/day during GD 10–GD 20 and 0.67 mg/kg body weight/day during PND 1–PND 20) [25]. In case of dams treated with 12 ppm PTU, intake value was 1.97 mg/kg body weight/day during the whole exposure period (1.54 mg/kg body weight/day during GD 10–GD 20 and 2.20 mg/kg body weight/day during PND 1–PND 20). In case of dams treated with 200 ppm MMI, intake value was 27.2 mg/kg body weight/day during the whole exposure period (19.7 mg/kg body weight/day during GD 10–GD 20 and 31.2 mg/kg body weight/day during PND 1–PND 20).

3.2. Effects on offspring growth and survival

With regard to the reproductive parameters, no significant alterations in the number of implantation sites, number of live offspring, and sex ratio were observed by the exposure to anti-thyroid agents. At PND 1, a slight and non-significant decrease of the body weight was observed in all exposure groups of both sexes [25]. All animals survived during the lactation period. At PND 20, a decrease of body weight was observed after exposure to anti-thyroid agents in both sexes, which was statistically significant in the males of the 12 ppm PTU and MMI groups and in females of all exposure groups. After weaning, four out of ten males and six out of ten females receiving 12 ppm PTU were found dead or subjected to moribund sacrifice. During observation, many of these animals were hyperactive and aggressive in nature and sometimes raced around to bump into a cage wall. During necropsy, most of these animals showed evidence of acute hemorrhage of the brain surface.

At the necropsy of 11-week rats, only six males and four females remained in the 12 ppm PTU group, whereas 10 animals/sex remained in other groups. Offspring of dams receiving 12 ppm PTU and MMI showed a statistically significant decrease in body weight in both sexes [25].

3.3. Serum levels of thyroid-related hormones

At PND 20, decreases of serum levels of T_3 and T_4 were evident in animals that were administered anti-thyroid agents with statistical significance in all groups of animals exposed to anti-thyroid agents for both T_3 and T_4 (Table 1). Reductions of T_3 and T_4 with PTU occurred in a dose-dependent fashion. Significantly elevated TSH levels were observed with MMI and PTU at both doses. At PNW 11, a slight but statistically significant decrease of T_3 levels was observed with MMI and 12 ppm PTU groups.

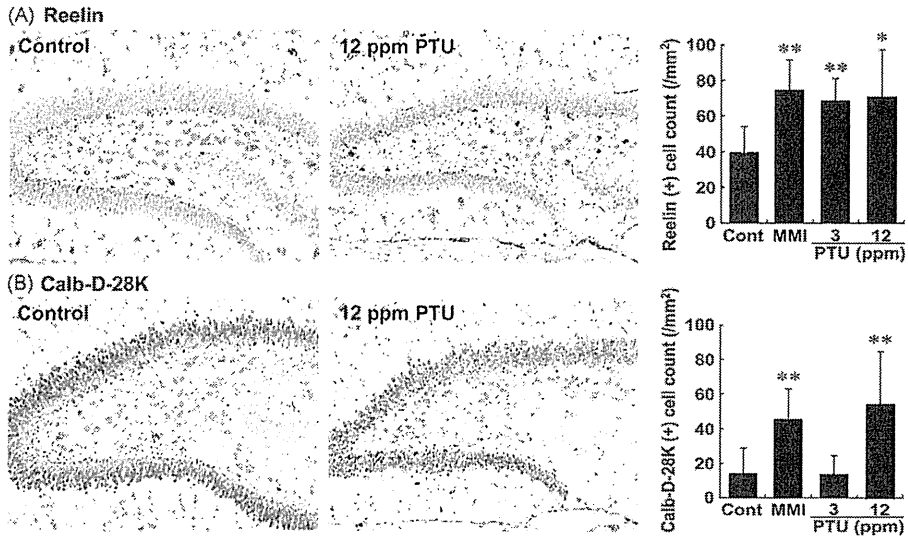

Fig. 2. Distribution of immunoreactive cells for Reelin and Calb-D-28K in the hippocampal formation in male rats at PND 20 after maternal exposure to anti-thyroid agents. (A) Reelin-immunoreactive cells in the hilus of the dentate gyrus. Reelin-positive cells with abundant cytoplasm show scattered distribution within the hilar region of the dentate gyrus. Note the higher number of Reelin-positive cells in a case exposed to 12 ppm PTU (Right) as compared with the control animal (Left). Magnification, 100×. The graph shows the number of Reelin-positive cells/unit area (mm^2) of the hilus of the bilateral hemispheres. $^{*}P<0.05$, $^{**}P<0.01$ *versus* untreated controls. (B) Calb-D-28K-immunoreactive cells in the hilus of the dentate gyrus. Calb-D-28K-positive cells are mainly distributed in the area medial to the subgranular zone. Note the higher number of Calb-D-28K-positive cells in a case exposed to 12 ppm PTU (Right) as compared with the control animal (Left). Magnification, 100×. The graph shows the number of Calb-D-28K-positive cells/unit area (mm^2) of the hilus of the bilateral hemispheres. $^{**}P<0.01$ *versus* untreated controls.

3.4. Immunolocalization of Reelin and Calb-D-28K in the hippocampal formation at PND 20

The distribution of Reelin-immunoreactive cells in the hippocampal formation that included the CA1–3 regions was similar to that described in the literature [14]. In the dentate gyrus, Reelin was expressed predominantly in the interneurons located in the hilus (polymorphic layer), whereas Reelin-containing neurons were sparse in the molecular layer (Fig. 2A). Morphometrically, the number of Reelin-positive cells in the dentate hilus was normalized in terms of unit area, and all of the animals exposed to MMI or PTU showed an increased number of Reelin-positive cells with a rather diffuse distribution within the hilus.

With regard to Calb-D-28K, the CA1 pyramidal neurons expressed this molecule with intense immunoreactivity in the inner pyramidal cells. Within the dentate gyrus, neurons in the granular cell layer showed strong immunoreactivity, while cells in the subgranular zone showed no expression (Fig. 2B). In addition to Reelin, Calb-D-28K-immunoreactive cells were frequently observed in the dentate hilus at the position medial to the subgranular zone. As compared with the untreated controls, animals exposed to MMI or 12 ppm PTU exhibited an increased number of Calb-D-28K-positive cells in the dentate hilus, while 3 ppm PTU did not show any change.

3.5. Immunolocalization of Reelin and Calb-D-28K in the hippocampal formation at PNW 11

On PNW 11, Reelin-immunoreactive cells showed similar distributions to those at PND 20 within the hippocampal formation, although the total number was reduced in the CA1–3 regions, by contrast to the comparable numbers in the dentate gyrus at PND 20. In the hilus of the dentate gyrus, the immunoreactive cells were increased in the MMI- and both doses of PTU-exposed animals (Fig. 3).

There were no cells immunoreactive for Calb-D-28K in the hippocampal formation in both untreated controls and MMI or PTU-exposed animals.

3.6. Characterization of the neuronal cell population in the dentate hilus

Within the hilus of the dentate gyrus, the number of NeuN-positive cells was apparently increased in the MMI- and both doses of PTU-exposed animals at PNW 11 as indicated by solid line in Fig. 4A.

The number of GAD67-positive cells in the animals treated with 12 ppm PTU tended to increase at PNW 11 compared with untreated controls, but was unchanged at PND 20 (Fig. 4B, C).

Evaluation of the co-localization of Reelin and NeuN in the dentate hilus at PNW 11 in untreated controls and 12 ppm PTU-exposed animals revealed that more than half of the Reelin-positive cells were weakly positive (±) or negative (−) for NeuN in the untreated controls, and 12 ppm PTU apparently increased this cell population (Fig. 4D).

3.7. Apoptotic and proliferating cell indices in the dentate subgranular zone

Apoptotic bodies were not found in the subgranular zone of the untreated controls at PND 20 (Fig. 5A). Also, no apoptotic bodies were detected after exposure to 3 ppm PTU at this time point. Although the number was very few, apoptotic bodies were increased after exposure to 12 ppm PTU. MMI-exposed animals also showed an increasing tendency in the number of apoptotic bodies. At PNW 11, no apoptotic bodies were detected in all cases including untreated controls, except for one apoptotic body detected in one case out of six untreated control animals.

With regard to the PCNA-immunoreactivity in the subgranular zone in untreated control animals, positive nuclei were sparsely observed at PND 20, and the number was decreased at PNW 11 (Fig. 5B). When the number of PCNA-immunoreactive nuclei was compared between the untreated controls and 12 ppm PTU, the latter decreased the number at PND 20. On the other hand, at PNW 11, no statistical difference was observed in the number of immunoreactive cells between the two groups.

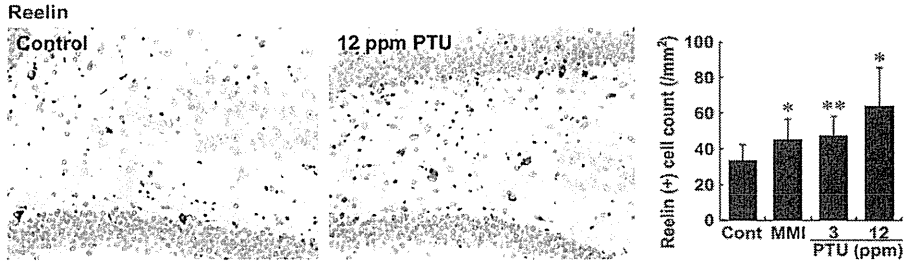

Fig. 3. Distribution of immunoreactive cells for Reelin in the hilus of the hippocampal dentate gyrus at PNW 11 of male rats exposed maternally to anti-thyroid agents. Similar to PND 20, the Reelin-positive cells with abundant cytoplasm show a scattered distribution within the hilar region of the dentate gyrus. Note the higher number of Reelin-positive cells in a case exposed to 12 ppm PTU (Right) as compared with the control animal (Left). Magnification, 100×. The graph shows the number of Reelin-positive cells/unit area (mm^2) of the hilus of the bilateral hemispheres. $^{*}P<0.05$, $^{**}P<0.01$ *versus* untreated controls.

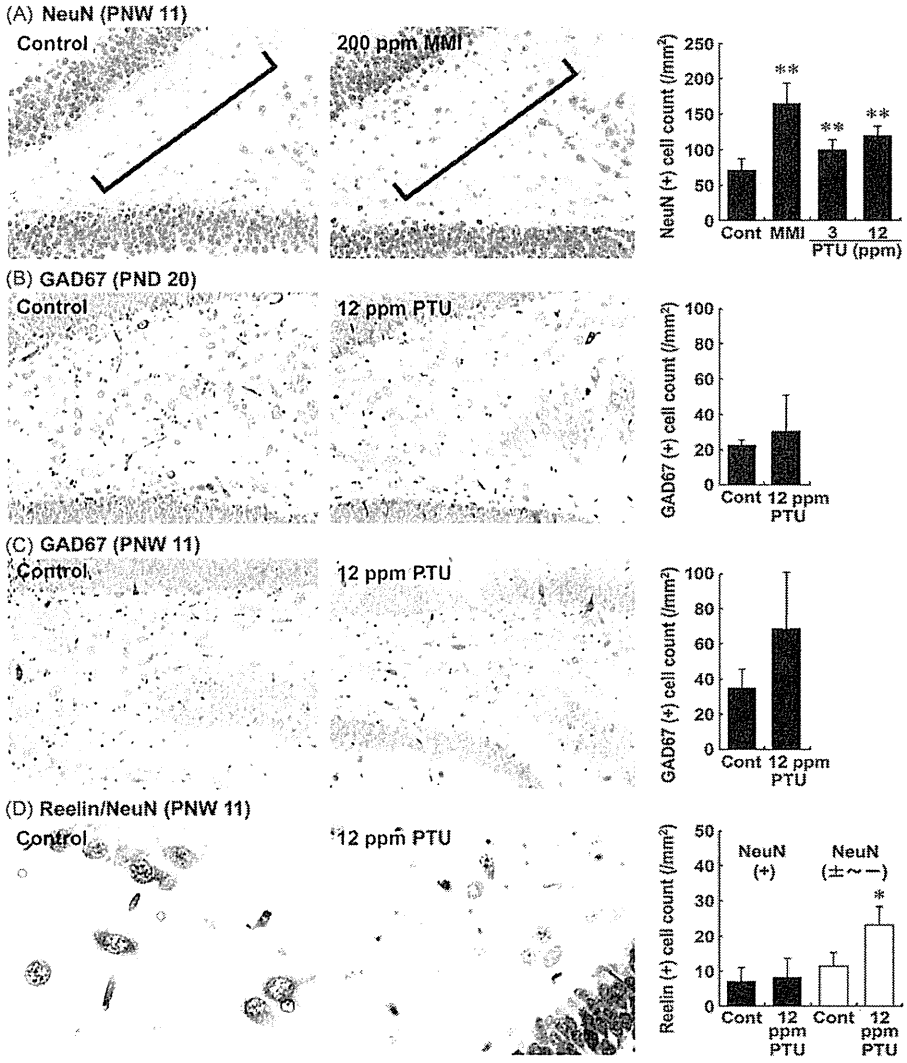

Fig. 4. Distribution of immunoreactive cells for NeuN and GAD67, and co-localization of Reelin and NeuN in the dentate hilus of male rats exposed maternally to anti-thyroid agents. (A) NeuN-immunoreactive cells at PNW 11. NeuN-positive cells are mainly distributed in the hilar area medial to the subgranular zone. Note the higher number of NeuN-positive cells in a case exposed to 200 ppm MMI (Right) as compared with the control animal (Left). Magnification, 200×. The graph shows the number of NeuN-positive cells/unit area (mm^2) of the hilus of the bilateral hemispheres. $^{**}P<0.01$ *versus* untreated controls. (B) GAD67-immunoreactive cells at PND 20. GAD67-positive cells with abundant cytoplasm show a scattered distribution within the hilar region. Magnification, 200×. Note there is no change in the number of GAD67-positive cells in a case exposed to 12 ppm PTU (Right) as compared with the control animal (Left). The graph shows the number of GAD67-positive cells/unit area (mm^2) of the hilus of bilateral hemispheres. (C) GAD67-immunoreactive cells at PNW 11. Similar to the PND 20 cases, the GAD67-positive cells with abundant cytoplasm show a scattered distribution within the hilar region. Magnification, 200×. Note the higher number of GAD67-positive cells in a case exposed to 12 ppm PTU (Right) as compared with the control animal (Left). The graph shows the number of GAD67-positive cells/unit area (mm^2) of the hilus of the bilateral hemispheres. (D) Double staining of Reelin and NeuN at PNW 11. Magnification, 600× (Left); 400× (Right). Note the increased number of Reelin-positive cells showing weak or no immunoreactivity for NeuN in a case exposed to 12 ppm PTU (Right) as compared with the control animal (Left). The graph shows the number of Reelin-positive cells with apparent (+) or weak to negative (±~−) NeuN-immunoreactivity/unit area (mm^2) of the hilus of the bilateral hemispheres. $^{*}P<0.01$ *versus* untreated controls.

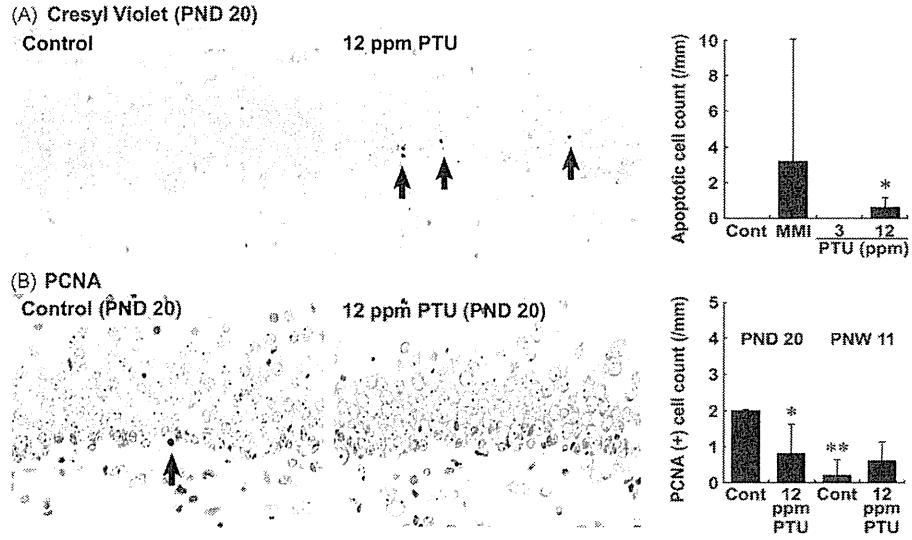

Fig. 5. Distribution of apoptotic cells and proliferating cells in the dentate subgranular zone of male rats exposed maternally to anti-thyroid agents. (A) Apoptotic cells detected as apoptotic bodies with Cresyl Violet staining at PND 20. Note sparse distribution of apoptotic bodies (arrows) in a case exposed to 12 ppm PTU (Right) as compared with the control animal without apoptotic bodies (Left). Magnification, 400×. The graph shows the number of apoptotic bodies/unit length (mm) of the subgranular zone of bilateral hemispheres at PND 20. $^{*}P < 0.05$ *versus* untreated controls. (B) Proliferating cells as detected by PCNA-positive nuclei at PND 20. Note one PCNA-positive nucleus (arrow) in the micrographic view of the control animal (Left), while no positive nuclei were found in a case of 12 ppm PTU (Right). Magnification, 400×. The graph shows the number of PCNA-positive nuclei/unit length (mm) of the subgranular zone of bilateral hemispheres at both PND 20 and PNW 11. $^{*}P < 0.05$, $^{**}P < 0.01$ *versus* untreated controls at PND 20.

4. Discussion

In our recent study using animals of the identical experiment of the present study, we detected typical hypothyroidism-related changes, such as thyroid follicular cell hypertrophy accompanied with increased thyroid weight, and fluctuations in the thyroid-related hormone levels at the end of maternal exposure to MMI or PTU [25]. Morphometrical analysis at the adult stage also revealed hypothyroidism-related brain changes reflecting neuronal mismigration [10] and impaired oligodendroglial development [2], in both chemicals, with PTU showing dose-dependence. Offspring also displayed evidence of growth retardation lasting into the adult stage with MMI and PTU at 12 ppm. Dams in these groups exhibited reductions in food intake and water consumption during the lactation period suggestive of the relation to the growth suppression of offspring. On the other hand, offspring exposed to 3 ppm PTU also exhibited reduced body weights at weaning, with a statistically significant difference in females, without a concurrent reduction of food intake and water consumption of dams, suggesting that the reduced body weight was due to the development of hypothyroidism [32].

With regard to male offspring exposed to 3 ppm PTU, a clear increase in Reelin-expressing cells was evident at the end of developmental exposure with the magnitude similar to other treatment groups, while body weight reduction with 3 ppm PTU was weak and non-significant. Increase of Reelin-expressing cells continued until adult stage in this group, irrespective of the no reduction in the terminal body weight. These results may suggest that the increase in Reelin-expressing cells was the reflection of hypothyroidism-related brain effect rather than systemic growth retardation. We recently found that experimental undernutrition of offspring during GD 10–PND 21 utilizing a rat intrauterine growth restriction model did not change the number of Reelin-expressing cells until adult stage (Ohishi and Shibutani, unpublished data).

During early postnatal life, Reelin expression becomes established in a subpopulation of GABAergic interneurons in the dentate gyrus, with a high density in the hilus and along the base of the granule cell layer [16], where Reelin is maintained throughout adult life [14,15]. In the present study, we also found an increase in Calb-D-28K-immunoeactive cells, as with Reelin-positive cells, in the dentate hilus after exposure to anti-thyroid agents at PND 20. Calcium binding protein Calb-D-28K and parvalbumin are known to form distinct subpopulations of GABAergic interneurons in the rodent hippocampal formation [33]. During early postnatal development in human, subpopulations of Reelin-positive interneurons express Calb-D-28K in the dentate hilus [34]. These results suggest that the increased Reelin-expressing cells in the dentate hilus at the end of developmental hypothyroidism in the present study are GABAergic interneurons. However, the Calb-D-28K-expressing cells disappeared at the adult stage, regardless of the presence of Reelin-expressing cells in the present study. Because aged rats lack Calb-D-28K expression in the hippocampal interneurons [35], Calb-D-28K may play a role in functional maturation of these cells [36]. Interestingly, experimental induction of epileptic seizures in rats facilitates neurogenesis of cells expressing Calb-D-28K in the dentate hilus [37,38].

In the adult stage, we also found increased numbers of Reelin-positive cells and NeuN-positive cells in the dentate hilus after developmental exposure to anti-thyroid agents. In parallel with the increase in NeuN-positive cells, the increased GAD67-positive population was confirmed in the 12 ppm PTU-exposed animals. On the other hand, double staining of Reelin and NeuN revealed that developmental hypothyroidism resulted in an increase in Reelin-positive cells showing weakly positive or negative NeuN-immunoreactivity. Faint expression of mature neuronal markers, such as NeuN and microtubule-associated protein-2, was reported to reflect immature nature of neurons [39]. These results suggest that developmental hypothyroidism resulted in a sustained increase in GABAergic interneurons in the dentate hilus until the adult stage, a subpopulation of these cells produced Reelin with immature neuronal nature.

In line with its role in neuronal migration during development, Reelin was reported to be involved in the rostral migratory stream

in adult rats [40]. Hippocampal heterotopias seen after exposure to methylazoxymethanol during uterine life [41] are not observed at birth but become progressively more evident between P5 and P21. Similarly, developmental hypothyroidism induced subcortical band heterotopia at weaning (PND 20), and this becomes more evident at the adult stage [25]. Because Reelin acts as a stop signal [42], postnatal overexpression of Reelin in the dentate hilus in the present study could be responsible for heterotopias by maintaining the migrating granular cells in an incorrect position.

On the other hand, the transient prenatal disturbance of neurogenesis by treatment with methylazoxymethanol induces a long-term increase in the number of neurons expressing Reelin in the hippocampus [43]. In the dentate gyrus, the neuronal stem/progenitor cells are located within the subgranular zone, and neurogenesis occurs constitutively throughout postnatal life in adult mammals [44]. During postnatal hypothyroidism, neural progenitor proliferation and differentiation have been shown to be impaired [3]. In the present study, we found a slight increase or increasing tendency in apoptotic cells as well as a slight suppression of cell proliferation activity in the dentate subgranular zone at PND 20 at the end of exposure to anti-thyroid agents, while these changes were not continued until adult stage. Similar supportive data have recently been reported showing gene expression changes suggestive of facilitation of apoptosis and suppression of cell proliferation in the hippocampal formation during the postnatal hypothyroidism and down-regulation of anti-apoptotic genes at the adult stage [20]. Thus, although the reason and consequence of overexpression of Reelin during adulthood is unclear, Reelin production can be sustained in later life in response to impaired neurogenesis as with mismigration in the dentate granular cells during development, and interneurons may play a role in sustained Reelin production. It is suggested that GABAergic inputs to dentate progenitor cells in adult stage promote activity-dependent neuronal differentiation [45].

5. Conclusions

In this study, we have shown persistent increases in GABAergic interneurons with Reelin production in an immature population until the adult stage in the dentate hilus after developmental hypothyroidism. These findings probably reflect a compensatory regulation for impaired neurogenesis and mismigration. There are many xenobiotic chemicals having a potential to interfere with thyroid hormone signaling in the developing brain. Considering an increasing demand to develop efficient screening method of developmental neurotoxicants, monitoring of Reelin-expressing interneurons in the hippocampal dentate hilus may provide a valuable tool for detection of chemicals that can affect neurogenesis and migration.

Conflict of interest

All of the authors disclose that there are no conflicts of interest that could inappropriately influence the outcomes of the present study.

Acknowledgments

We thank Miss Tomomi Morikawa for her technical assistance in conducting the animal study. We also thank Mrs. Shigeko Suzuki and Miss Ayako Kaneko for their technical assistance in preparing the histological specimens. This work was supported in part by Health and Labour Sciences Research Grants (Research on Risk of Chemical Substances) from the Ministry of Health, Labour and Welfare of Japan.

References

[1] Porterfield SP. Thyroidal dysfunction and environmental chemicals—potential impact on brain development. Environ Health Perspect 2000;108:433–8.
[2] Schoonover CM, Seibel MM, Jolson DM, Stack MJ, Rahman RJ, Jones SA, et al. Thyroid hormone regulates oligodendrocyte accumulation in developing rat brain white matter tracts. Endocrinology 2004;145:5013–20.
[3] Montero-Pedrazuela A, Venero C, Lavado-Autric R, Fernández-Lamo I, García-Verdugo JM, Bernal J, et al. Modulation of adult hippocampal neurogenesis by thyroid hormones: implications in depressive-like behavior. Mol Psychiatry 2006;11:361–71.
[4] de Escobar GM, Obregón MJ, del Rey FE. Iodine deficiency and brain development in the first half of pregnancy. Public Health Nutr 2007;10:1554–70.
[5] Asplund L, Svensson B, Eriksson U, Jansson B, Jensen S, Wideqvist U, et al. PCBs, DDT, DDE in human plasma related to fish consumption. Arch Environ Health 1994;49:477–86.
[6] Kodavanti PR, Ward TR, Derr-Yellin EC, Mundy WR, Casey AC, Bush B, et al. Congener-specific distribution of PCBs in brain regions, blood, liver, and fat of adult rats following repeated exposure to Aroclor 1254. Toxicol Appl Pharmacol 1998;153:199–210.
[7] Langer P. Review: persistent organochlorinated pollutants (POPs) and human thyroid—2005. Endocr Regul 2005;39:53–68.
[8] Comer CP, Norton S. Effects of perinatal methimazole exposure on a developmental test battery for neurobehavioral toxicity in rats. Toxicol Appl Pharmacol 1982;63:133–41.
[9] Akaike M, Kato N, Ohno H, Kobayashi T. Hyperactivity and spatial maze learning impairment of adult rats with temporary neonatal hypothyroidism. Neurotoxicol Teratol 1991;13:317–22.
[10] Lavado-Autric R, Ausó E, García-Velasco JV, Arufe Mdel C, del Rey FE, Berbel P, et al. Early maternal hypothyroxinemia alters histogenesis and cerebral cortex cytoarchitecture of the progeny. J Clin Invest 2003;111:954–7.
[11] Goodman JH, Gilbert ME. Modest thyroid hormone insufficiency during development induces a cellular malformation in the corpus callosum: a model of cortical dysplasia. Endocrinology 2007;148:2593–7.
[12] D'Arcangelo G, Miao GG, Chen SC, Soares HD, Morgan JI, Curran T. A protein related to extracellular matrix proteins deleted in the mouse mutant reeler. Nature 1995;374:719–23.
[13] D'Arcangelo G, Nakajima K, Miyata T, Ogawa M, Mikoshiba K, Curran T. Reelin is a secreted glycoprotein recognized by the CR-50 monoclonal antibody. J Neurosci 1997;17:23–31.
[14] Pesold C, Impagnatiello F, Pisu MG, Uzunov DP, Costa E, Guidotti A, et al. Reelin is preferentially expressed in neurons synthesizing γ-aminobutyric acid in cortex and hippocampus of adult rats. Proc Natl Acad Sci USA 1998;95:3221–6.
[15] Scotti AL, Herrmann G. Reelin immunoreactivity in dissociated cultures of the postnatal hippocampus. Brain Res 2002;924:209–18.
[16] Houser CR. Interneurons of the dentate gyrus: an overview of cell types, terminal fields and neurochemical identity. Prog Brain Res 2007;163:217–32.
[17] Alvarez-Dolado M, Ruiz M, Del Río JA, Alcántara S, Burgaya F, Sheldon M, et al. Thyroid hormone regulates reelin and dab1 expression during brain development. J Neurosci 1999;19:6979–93.
[18] Lussier AL, Caruncho HJ, Kalynchuk LE. Repeated exposure to corticosterone, but not restraint, decreases the number of reelin-positive cells in the adult rat hippocampus. Neurosci Lett 2009;460:170–4.
[19] Gong C, Wang TW, Huang HS, Parent JM. Reelin regulates neuronal progenitor migration in intact and epileptic hippocampus. J Neurosci 2007;27:1803–11.
[20] Zhang L, Blomgren K, Kuhn HG, Cooper-Kuhn CM. Effects of postnatal thyroid hormone deficiency on neurogenesis in the juvenile and adult rat. Neurobiol Dis 2009;34:366–74.
[21] Glass CK, Holloway JM, Devary OV, Rosenfeld MG. The thyroid hormone receptor binds with opposite transcriptional effects to a common sequence motif in thyroid hormone and estrogen response elements. Cell 1988;54:313–23.
[22] Zhu YS, Yen PM, Chin WW, Pfaff DW. Estrogen and thyroid hormone interaction on regulation of gene expression. Proc Natl Acad Sci USA 1996;93:12587–92.
[23] Masutomi N, Shibutani M, Takagi H, Uneyama C, Takahashi N, Hirose M. Impact of dietary exposure to methoxychlor, genistein, or diisononyl phthalate during the perinatal period on the development of the rat endocrine/reproductive systems in later life. Toxicology 2003;192:149–70.
[24] Hopert AC, Beyer A, Frank K, Strunck E, Wunsche W, Vollmer G. Characterization of estrogenicity of phytoestrogens in an endometrial-derived experimental model. Environ Health Perspect 1998;106:581–6.
[25] Shibutani M, Woo G-H, Fujimoto H, Saegusa Y, Takahashi M, Inoue K, et al. Assessment of developmental effects of hypothyroidism in rats from in utero and lactation exposure to anti-thyroid agents. Reprod Toxicol 2009;28:297–307.
[26] Barradas PC, Vieira RS, De Freitas MS. Selective effect of hypothyroidism on expression of myelin markers during development. J Neurosci Res 2001;66:254–61.
[27] Sawin S, Brodish P, Carter CS, Stanton ME, Lau C. Development of cholinergic neurons in rat brain regions: dose-dependent effects of propylthiouracil-induced hypothyroidism. Neurotoxicol Teratol 1998;20:627–35.
[28] Sui L, Anderson WL, Gilbert ME. Impairment in short-term but enhanced long-term synaptic potentiation and ERK activation in adult hippocampal area CA1 following developmental thyroid hormone insufficiency. Toxicol Sci 2005;85:647–56.

[29] Nakamura R, Teshima R, Hachisuka A, Sato Y, Takagi K, Nakamura R, et al. Effects of developmental hypothyroidism induced by maternal administration of methimazole or propylthiouracil on the immune system of rats. Int Immunopharmacol 2007;7:1630–8.
[30] Shibutani M, Lee K-Y, Igarashi K, Woo G-H, Inoue K, Nishimura T, et al. Hypothalamus region-specific global gene expression profiling in early stages of central endocrine disruption in rat neonates injected with estradiol benzoate or flutamide. Dev Neurobiol 2007;67:253–69.
[31] Nuñez JL, McCarthy MM. Cell death in the rat hippocampus in a model of prenatal brain injury: time course and expression of death-related proteins. Neuroscience 2004;129:393–402.
[32] Hapon MB, Simoncini M, Via G, Jahn GA. Effect of hypothyroidism on hormone profiles in virgin, pregnant and lactating rats, and on lactation. Reproduction 2003;126:371–82.
[33] Seress L, Gulyás AI, Ferrer I, Tunon T, Soriano E, Freund TF. Distribution, morphological features, and synaptic connections of parvalbumin- and calbindin D28k-immunoreactive neurons in the human hippocampal formation. J Comp Neurol 1993;337:208–30.
[34] Abraham H, Meyer G. Reelin-expressing neurons in the postnatal and adult human hippocampal formation. Hippocampus 2003;13:715–27.
[35] Potier B, Krzywkowski P, Lamour Y, Dutar P. Loss of calbindin-immunoreactivity in CA1 hippocampal stratum radiatum and stratum lacunosum-moleculare interneurons in the aged rat. Brain Res 1994;661: 181–8.
[36] Grateron L, Cebada-Sanchez S, Marcos P, Mohedano-Moriano A, Insausti AM, Muñoz M, et al. Postnatal development of calcium-binding proteins immunoreactivity (parvalbumin, calbindin, calretinin) in the human entorhinal cortex. J Chem Neuroanat 2003;26:311–6.
[37] Scharfman HE, Goodman JH, Sollas AL. Granule-like neurons at the hilar/CA3 border after status epilepticus and their synchrony with area CA3 pyramidal cells: unctional implications of seizure-induced neurogenesis. J Neurosci 2000;20:6144–58.
[38] Scharfman HE, Solias AL, Goodman JH. Spontaneous recurrent seizures after pilocarpine-induced status epilepticus activate calbindin-immunoreactive hilar cells of the rat dentate gyrus. Neuroscience 2002;111:71–81.
[39] Seki T. Expression patterns of immature neuronal markers PSA-NCAM, CRMP-4 and NeuroD in the hippocampus of young adult and aged rodents. J Neurosci Res 2002;70:327–34.
[40] Hack I, Bancila M, Loulier K, Carroll P, Cremer H. Reelin is a detachment signal in tangential chain-migration during postnatal neurogenesis. Nat Neurosci 2002;5:939–45.
[41] Baraban SC, Wenzel HJ, Hochman DW, Schwartzkroin PA. Characterization of heterotopic cell clusters in the hippocampus of rats exposed to methylazoxymethanol in utero. Epilepsy Res 2000;39:87–102.
[42] Frotscher M, Haas CA, Förster E. Reelin controls granule cell migration in the dentate gyrus by acting on the radial glial scaffold. Cereb Cortex 2003;13:634–40.
[43] Hoareau C, Hazane F, Le Pen G, Krebs MO. Postnatal effect of embryonic neurogenesis disturbance on reelin level in organotypic cultures of rat hippocampus. Brain Res 2006;1097:43–51.
[44] von Bohlen U, Halbach O. Immunohistological markers for staging neurogenesis in adult hippocampus. Cell Tissue Res 2007;329:409–20.
[45] Tozuka Y, Fukuda S, Namba T, Seki T, Hisatsune T. GABAergic excitation promotes neuronal differentiation in adult hippocampal progenitor cells. Neuron 2005;47:803–15.

International Immunopharmacology 10 (2010) 393–397

Contents lists available at ScienceDirect

International Immunopharmacology

journal homepage: www.elsevier.com/locate/intimp

Effects of tetrabromobisphenol A, a brominated flame retardant, on the immune response to respiratory syncytial virus infection in mice

Wataru Watanabe [a], Tomomi Shimizu [b], Rie Sawamura [b], Akane Hino [b], Katsuhiko Konno [c], Akihiko Hirose [d], Masahiko Kurokawa [b,*]

[a] Department of Microbiology, School of Pharmaceutical Sciences, Kyushu University of Health and Welfare, Yoshino 1714-1, Nobeoka, Miyazaki 882-8508, Japan
[b] Department of Biochemistry, School of Pharmaceutical Sciences, Kyushu University of Health and Welfare, Yoshino 1714-1, Nobeoka, Miyazaki 882-8508, Japan
[c] Department of Clinically Veterinary Medicine, School of Pharmaceutical Sciences, Kyushu University of Health and Welfare, Yoshino 1714-1, Nobeoka, Miyazaki 882-8508, Japan
[d] Division of Risk Assessment, Biological Safety Research Center, National Institute of Health Sciences, 1-18-1, Kamiyoga, Setagaya-ku, Tokyo 158-8501, Japan

ARTICLE INFO

Article history:
Received 1 December 2009
Accepted 28 December 2009

Keywords:
Respiratory syncytial virus
Tetrabromobisphenol A
Pneumonia
Cytokines
Double-positive CD4+CD8+ cells

ABSTRACT

Effects of the brominated flame retardants (BFRs), decabrominated diphenyl ether (DBDE), hexabromocyclododecane (HBCD), and tetrabromobisphenol A (TBBPA), on host immunity of mice were evaluated using respiratory syncytial virus (RSV) infection. Five-week-old female mice were fed a diet containing 1% BFRs for 28 days, and subsequently infected with RSV. No toxicological sign was observed in BFR-treated mice before infection. TBBPA significantly increased the pulmonary viral titer in the infected mice on day 5 post-infection, but DBDE and HBCD did not. Slight histological changes were observed in lung tissues of TBBPA-treated mice with mock infection. These changes due to TBBPA were much exacerbated by RSV infection. Cytokine analysis of bronchoalveolar lavage fluid (BALF) from RSV-infected mice treated with or without TBBPA revealed that TBBPA significantly increased the levels of tumor necrosis factor (TNF)-α, interleukin (IL)-6 and interferon (IFN)-γ at each time point after virus infection, but no change was observed for IL-1β and IL-12. The levels of IL-4 and IL-10, Th2 cytokines, significantly decreased. Thus, TBBPA caused unusual production of the various cytokines in RSV-infected mice. Flow cytometry revealed that the percentage of double-positive CD4+CD8+ cells, immature T lymphocytes, in the cell populations in BALF from RSV-infected mice increased due to TBBPA treatment. The change was not observed in spleen cells of TBBPA-treated mice. The response to RSV infection verified that TBBPA treatment affected the host immunity of mice. Irregular changes in cytokine production and immune cell populations due to TBBPA treatment were suggested to cause exacerbation of pneumonia in RSV-infected mice.

1. Introduction

Human respiratory syncytial virus (RSV), a member of the family *Paramyxoviridae*, is the most prevalent infectious agent of acute lower respiratory illness in infants and young children [1]. Infection and reinfection with RSV are frequent during the first few years of life, and most children are infected by 24 months of age [2]. Clinically severe RSV infection is seen primarily in young children with naïve immune systems and/or genetic predispositions [3], patients with suppressed T-cell immunity [1], and the elderly [4]. A murine model of RSV infection has been used to develop anti-viral drugs and vaccines [5]. In this murine model, the development of pneumonia reflects the severity of RSV infection, and the pneumonia is histopathologically similar to that in humans [6,7]. We previously demonstrated that the severity of the RSV infection significantly reflected the host immune condition [8]. This RSV infection mouse model was shown to be useful to evaluate the immunotoxicity of chemical compounds [9].

Recently, it was reported that long-term exposure to industrial compounds containing brominated flame retardants (BFRs) may be toxic to humans, especially infants and children [10]. There are five major BFRs, tetrabromobisphenol A (TBBPA), hexabromocyclododecane (HBCD), and three commercial mixtures of polybrominated diphenyl ethers (PBDEs), which are known as decabromodiphenyl ether (DBDE), octabromodiphenyl ether (OBDE), and pentabromodiphenyl ether (pentaBDE). They are used as additive or reactive components in a variety of polymers, such as polystyrene foams, high-impact polystyrene, and epoxy resins [10]. BFRs are ubiquitously used as industrial materials worldwide. TBBPA accounted for approximately 76% of the BFRs consumed in Asia in 2001, and the amount used was approximately 90,000 tons [10]. BFRs are easily released into an environment due to deterioration or abrasion of the materials, but there is limited knowledge about their effects on health, particularly their effects on the immune systems of mammals [11–13]. To evaluate human health damage due to this environmental contaminant, the

* Corresponding author. Tel.: +81 982 23 5578; fax: +81 982 23 5684.
E-mail address: b2mk@phoenix.ac.jp (M. Kurokawa).

1567-5769/$ – see front matter © 2010 Elsevier B.V. All rights reserved.
doi:10.1016/j.intimp.2009.12.014

mechanism of action of BFRs on the immune system needs to be clarified.

In this study, the effects of DBDE, HBCD and TBBPA on host immunity were comparatively evaluated using the RSV infection mouse model.

2. Materials and methods

2.1. Mice

Female (4 weeks old) BALB/c mice were purchased from Kyudo Animal Laboratory (Kumamoto, Japan) and housed at 25 ± 2 °C. The mice were allowed free access to a conventional solid diet CRF-1 (Oriental Yeast Co., Chiba, Japan) and water and used in this experiment after 7 days acclimation. The animal experimentation guideline of the Kyushu University of Health and Welfare was followed in the animal studies.

2.2. Cells and virus

Human epidermoid carcinoma (HEp-2) cells (American Type Culture Collection CCL-23) were purchased from Dainippon Pharmaceutical (Osaka, Japan) and maintained in Eagle's minimum essential medium supplemented with heat-inactivated 10% fetal calf serum (FCS). The A2 strain of RSV was obtained from American Type Culture Collection (Rockville, MD) and grown in HEp-2 cell cultures. Viral titers of HEp-2 cells were measured by the plaque method, and expressed as plaque-forming units per milliliter (PFU/ml) [8].

2.3. BFRs

DBDE was purchased from Wako Pure Chemicals (Osaka, Japan). HBCD and TBBPA were purchased from Tokyo Kasei (Tokyo, Japan). They were mixed into a powder diet, which was soy-free to avoid the estrogen-like effect of soybeans, based on the formulation of the NIH-07 open-formula rodent diet [14] and produced by Oriental Yeast Co (Chiba, Japan).

2.4. Animal tests

Five-week-old female mice were fed a soy-free diet mixed with 1% DBDE, HBCD or TBBPA for 4 weeks. After treatment, these mice were fed CRF-1 and used for the following RSV infection test. Throughout the experiments, both chows and drinking water were given ad libitum.

The RSV infection test was performed as reported previously [9]. Briefly, 9-week-old female mice were infected intranasally with 1×10^6 or 1×10^5 PFU per 0.1 ml of the A2 strain of RSV under anesthesia. Mock-infected mice were also inoculated intranasally with 0.1 ml of phosphate-buffered saline (PBS) under anesthesia. On days 1, 3, 5 and 7 after infection, bronchoalveolar lavage fluid (BALF) was obtained from the mice under anesthesia by instilling of 1.0 ml of cold PBS into the lungs and aspirating it from the trachea using a tracheal cannula [15]. Ice-cold BALF was centrifuged at 100 × *g* at 4 °C for 10 min. After centrifugation, the supernatant was stored at −80 °C until to use. The cell pellet was suspended in PBS on ice and used as bronchoalveolar lavage (BAL) cells. For virus titration, the lungs were removed on day 5 post-infection, immediately frozen in liquid N_2, and stored at −80 °C. Frozen lung tissue was homogenized with cold quartz sand in a homogenizer, and viral titers in the supernatants of the homogenates were measured by a plaque assay [8]. The spleen was removed and minced by a scissor to obtain the cell suspension. A single cell suspension of spleen in ice-cold PBS was prepared by the filtration through a sterilized nylon-mesh.

2.5. Histological methods

For histological examination of the infected lungs, mock- or RSV-infected mice were sacrificed on day 5 post-infection, and lungs were removed and placed in buffered formalin for a minimum of 24 h. The tissue was then embedded in low-melting point paraffin, sectioned at a thickness of 5 μm, and stained with hematoxylin and eosin.

2.6. ELISA

Interleukin (IL)-1β, IL-4, IL-6, IL-10, interferon (IFN)-γ and tumor necrosis factor (TNF)-α levels in BALF were measured using specific ELISA kits (Ready-set-go, eBioscience Inc., San Diego, CA) according to the manufacturer's instructions. IL-12 levels in BALF were also measured using a specific kit (Ready-set-go, eBioscience Inc.) for IL-12 p70, without interference by p40 monomer or the related protein IL-23, according to the manufacturer's instructions. These products were tested and found to conform to all eBioscience Inc. quality control release specifications. The lower limits of detection sensitivity in the kits are 8 (pg/mL) for IL-1β, 4 (pg/mL) for IL-4, 4 (pg/mL) for IL-6, 8 (pg/mL) for IL-10, 15 (pg/mL) for IL-12 p70, 4 (pg/mL) for IFN-γ, and 8 (pg/mL) for TNF-α. The intra- and inter-assay coefficients of variation for these ELISA were less than 10%.

2.7. Flow cytometric analysis of BAL and spleen cells

Two-color analysis of BAL cells and spleen cells was performed using a FACS Calibur 3S flow cytometer (Becton Dickinson, Sunnyvale, CA). The following antibodies were used for phenotyping of murine cells: phycoerythrin (PE)-labeled hamster anti-CD3 (145-2C11), rat anti-CD8 (53.6), rat anti-CD11b (M1/70) and rat anti-CD49b (DX5) antibodies, fluorescein isothiocyanate (FITC)-labeled rat anti-CD4 (L3T4) and rat anti-CD25 (7D4) antibodies. All antibodies were purchased from BD Bioscience Pharmingen (San Diego, CA). Samples for analysis were prepared according to the manufacturer's instructions. Briefly, 0.05 ml of a single cell suspension (5×10^5 cells) in PBS was incubated with 0.02 ml of each PE-labeled antibody at 4 °C for 30 min. After incubation, the cells were washed with PBS and then incubated with 0.02 ml of each FITC-labeled antibody at 4 °C for 30 min. The cells were then washed as described above. After staining, at least 10,000 cells suspended in PBS on ice were analyzed by FACS. Finally, the data were analyzed with Cellquest software.

2.8. Statistical analysis

Comparisons of pulmonary viral titers and the levels of cytokines of the control and experimental groups were carried out using Student's *t*-test. A *P* value of 0.05 or less was considered to be significant.

3. Results

3.1. Effects of BFRs on RSV infection in mice

The effects of three BFRs on the severity of RSV infection in mice were investigated. Five-week-old female BALB/c mice were fed a diet containing 1% DBDE, HBCD, or TBBPA for 28 days. No loss of body weight at 28 day or decrease in food consumption during the treatment was detected in BFR-treated mice (Table 1). No particular toxicological sign, such as tremor, or abnormal behavior was observed in these mice either. Then, the mice were intranasally infected with

Table 1
Body weights and food consumption of DBDE-, HBCD- and TBBPA-treated mice.[a]

Index	Experiment 1			Experiment 2	
	Control	DBDE	HBCD	Control	TBBPA
Body weight (g)	20.8 ± 1.1	21.9 ± 1.2	21.2 ± 0.6	20.3 ± 1.1	19.6 ± 0.9
Food consumption (g/week)	25.7 ± 0.3	26.4 ± 0.5	26.8 ± 0.4	24.1 ± 4.1	25.1 ± 2.2

[a] Values represent mean ± standard deviation of 6–7 mice.

the A2 strain of RSV at 1×10^6 PFU. On day 5 after RSV infection, pulmonary viral titers were significantly ($P<0.001$) increased in TBBPA-treated mice compared with the control (Table 2). However, an obvious increase in the pulmonary viral titers was not observed in DBDE- or HBCD-treated mice. To confirm the effects of TBBPA on RSV infection, an additional group was instilled with a low titer (1×10^5 PFU) of RSV (Table 2). The pulmonary viral titers in low-titer TBBPA-treated mice were significantly ($P<0.05$) higher than those in control mice as well. Then, to investigate whether TBBPA directly promotes the growth of virus, the effect of TBBPA on the replication of RSV was tested in vitro using HEp-2 cell cultures, with the result that the compound did not affect the growth of RSV (data not shown). Thus, although BFRs did not show any apparent toxicity in mice in this study, TBBPA increased the RSV titers in the lung tissues of RSV-infected mice.

3.2. Effects of TBBPA on the development of pneumonia in RSV-infected mice

The effects of TBBPA ingestion on lung tissues of RSV-infected mice were analyzed histopathologically. While typical features of pneumonia such as infiltrations of lymphocytes and neutrophils due to RSV infection were observed on day 5 post-infection in mice treated with and without TBBPA (Fig. 1a, b), severely exacerbated pneumonia with expansion of the inflammation and hyperplasia of macrophages were found in the infected mice treated with TBBPA (Fig. 1b). In mock-infected mice, mild inflammation and congestion were observed in TBBPA-treated mice compared with the control (Fig. 1c, d). These results indicated that TBBPA caused mild immune injury in lung tissues and that the lesion was exacerbated to severe pneumonia by RSV infection in mice.

3.3. Effects of TBBPA on levels of cytokines in BALF from RSV-infected mice

To investigate the effects of TBBPA on the immune system, the levels of various cytokines in BALF induced by RSV infection in mice treated with TBBPA were measured by ELISA on day 1, 3, 5 and 7 post-infection (Table 3). The levels of IFN-γ, a representative marker of pneumonia due to RSV infection, in BALF from TBBPA-treated mice were significantly ($P<0.01$) increased and approximately 5.2-fold of the control on day 5 post-infection. IFN-γ could not be detected in BALF from mock-infected mice with or without TBBPA treatment (data not shown). On day 1 post-infection, the levels of both TNF-α and IL-6 in TBBPA-treated mice were significantly ($P<0.05$) increased to 5.8- and 2.6 times, respectively, of the control. No significant increase of IL-1β or IL-12 was found after TBBPA treatment. In contrast to these results, the levels of both IL-4 and IL-10, Th2 cytokines, were significantly ($P<0.05$) reduced on day 7 post-infection in BALF from TBBPA-treated mice compared with the control. Thus, TBBPA treatment enhanced production of TNF-α, IL-6 and IFN-γ but suppressed production of IL-4 and IL-10 in RSV-infected mice.

3.4. Effect of TBBPA on cell populations in BAL and spleen cells in RSV-infected mice

To clarify the effects of TBBPA on immune responses in RSV-infected mice, the cell populations of BAL and spleen cells were analyzed on days 1 and 3 post-infection by flow cytometry (Table 4). There were no significant differences in the number of BAL cells in control and TBBPA-treated mice groups in RSV-infected mice (data not shown). On day 1 post-infection, CD11b+ (positive) cells, dendritic cells or macrophages, accounted for more than 90% of BAL cells, and a difference in the population ratios of the control and TBBPA-treated mice was not observed. However, the percentages of double-positive T cells (CD4+CD8+), immature T cells, were markedly increased in BAL cells from RSV-infected mice due to treatment with TBBPA on day 3 post-infection, although there was no difference the number of CD4+CD8+ cells in mock-infected mice. The percentages of CD49b+ cells, NK cells, in BAL cells on days 1 and 3 post-infection were not affected by treatment with TBBPA. Although TBBPA reduced the ratio of CD3+CD25+ cells, activated T cells, on day 1 post-infection, they were low overall in BALF from RSV-infected mice. To evaluate the effects of TBBPA treatment on systemic immunity, CD11b+ and CD4+CD8+ cells in spleens of mock- and RSV-infected mice were analyzed on day 3 post-infection, but no difference due to TBBPA treatment was observed in the treated mice.

4. Discussion

To evaluate the effects of three BFRs on the host immunity of mice, a murine RSV infection model was used in this study [8,9]. Although mice were fed a diet containing 1% BFR for 4 weeks, no toxicity was observed in the BFR-treated mice (Table 1). The dosage of BFRs based on the average food consumption and body weight was calculated at approximately 1700 mg/kg/day (Table 1). The dosage sounds very high, but these BFRs were reported to be non-toxic in mice at this dosage for this treatment period [16,17], and our results were consistent with the reports. However, a significant ($P<0.001$) increase of pulmonary viral titers was detected in TBBPA-treated mice compared with the control, but not in DBDE- or HBCD-treated mice (Table 2). Consequently, it was verified that TBBPA treatment enhanced RSV growth in the lungs of mice.

In a histopathological analysis, mild lesions of the lungs were detected after TBBPA treatment in mock-infected mice (Fig. 1). Moreover, the administration of TBBPA was shown clearly to increase virus titers in the lungs (Table 2) and exacerbate the pneumonia in RSV-infected mice. Previously, treatment with an immunosuppressive agent, cyclophosphamide, was shown to increase pulmonary viral titers and exacerbate the pneumonia in RSV-infected mice [5,8]. This suggests that immune conditions in the host contribute to pulmonary virus titers and exacerbation of pneumonia. Thus, TBBPA might induce a disorder of the immunity against RSV infection, resulting in the increase of virus titers and exacerbation of pneumonia.

To clarify the immune disorder due to TBBPA administration, cytokine productions induced by RSV infection were examined (Table 3). In TBBPA-treated mice, marked increases of IL-6 and TNF-α were observed on day 1 post-infection. It was reported that these cytokines increase immediately in the early phase after RSV infection [18,19]. On the other hand, productions of IL-1β and IL-12, which are produced mainly by macrophages and dendritic cells, were not affected by TBBPA. As reported previously [8,9], the levels of IFN-γ, a marker of pneumonia, increased maximally on day 5 post-infection in RSV-infected mice, and its production was enhanced in TBBPA-treated mice (Table 3). The increase of IFN-γ may be induced by the increased IL-6 and TNF-α. Thus, these irregular cytokine productions indicate

Table 2
Effects of treatment of DBDE, HBCD and TBBPA on pulmonary viral titers on day 5 post-infection in RSV-infected mice.[a]

Group/BFRs treatment	Pulmonary viral titers (PFU/ml)		
	Experiment 1	Experiment 2	Experiment 3
Control	14,833 ± 8,566	17,433 ± 3,670	526 ± 146
DBDE	19,111 ± 18,000	ND	ND
HBCD	13,875 ± 2,776	ND	ND
TBBPA	ND	34,967 ± 7742**	1630 ± 764*

*Statistically different from control at $P<0.05$ (Student's t-test).
**Statistically different from control at $P<0.001$ (Student's t-test).
[a] Values represent mean ± standard deviation of 6–7 mice. Mice were infected intranasally with 1×10^6 PFU of RSV in experiments 1 and 2, and with 1×10^5 PFU in experiment 3. ND, not determined.

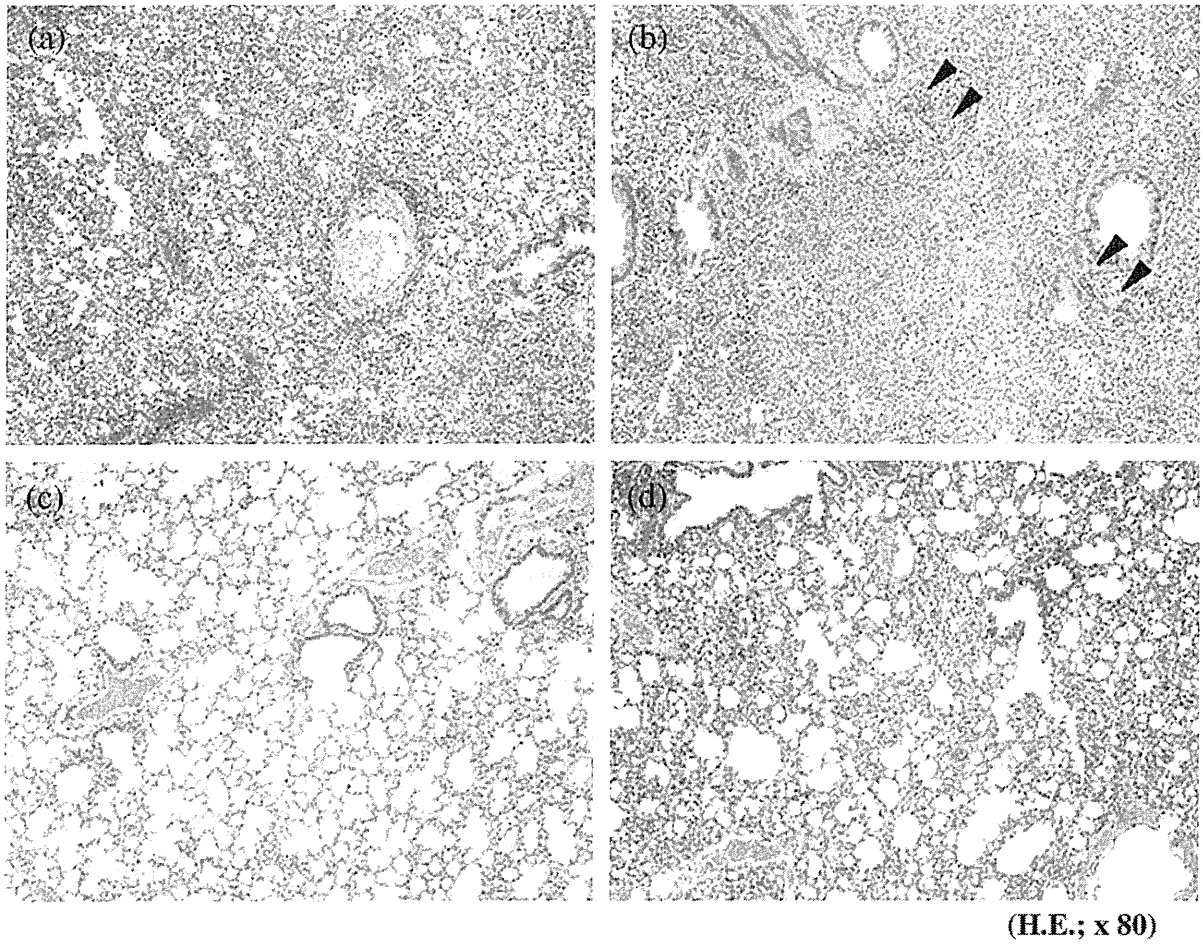

Fig. 1. Lungs of mice 5 days after mock or RSV infection. In this experiment, 4–5 mice per group were used, and representative data are shown. Arrowheads indicate macrophage hyperplasia. (a) Control mouse with RSV infection. (b) TBBPA-treated mouse with RSV infection. (c) Control mouse with mock infection. (d) TBBPA-treated mouse with mock infection. Hematoxylin and eosin stain.

that TBBPA caused disorder of the immune system in RSV-infected mice. Because the MAP kinases and protein kinase C were reported to be activated by TBBPA [20,21], disorder of the signal transduction system may be involved in the unusual production of the cytokines. On day 7 post-infection, IL-4 and IL-10, Th2 cytokines, were decreased in TBBPA-treated mice (Table 3). Studies for the development of a vaccine demonstrated that an imbalance of Th1/2 cytokines in the immune system is involved in the severity of RSV-induced disease [22]. Because TBBPA treatment strongly enhanced the production of

Table 3
Effects of TBBPA on cytokine concentration in BALF from RSV-infected mice.[a]

	Day 1 pi		Day 3 pi		Day 5 pi		Day 7 pi	
Cytokine	Control	TBBPA	Control	TBBPA	Control	TBBPA	Control	TBBPA
TNF-α	0.25 (0.17)	1.44* (0.74)	0.11 (0.02)	0.14 (0.03)	ND	ND	ND	ND
IL-1β	<0.04	0.05 (0.01)	ND	ND	ND	ND	ND	ND
IL-6	0.40 (0.14)	1.05** (0.06)	<0.02	<0.02	ND	ND	ND	ND
IL-12	0.11 (0.01)	0.15 (0.05)	0.15 (0.01)	0.18 (0.04)	ND	ND	ND	ND
IFN-γ	0.12 (0.02)	0.22 (0.07)	0.16 (0.02)	0.21 (0.07)	1.08 (0.86)	5.57** (2.82)	3.16 (2.66)	2.38 (0.99)
IL-4	ND	ND	<0.02	<0.02	0.04 (0.01)	0.03 (0.01)	0.06 (0.01)	0.04** (0.01)
IL-10	ND	ND	<0.08	<0.08	0.09 (0.02)	0.07 (0.02)	0.16 (0.02)	0.13* (0.01)

*Statistically different from control at $P<0.05$ (Student's t-test). **Statistically different from control at $P<0.01$ (Student's t-test).

[a] Concentration (ng/ml) of each cytokine in BALF from RSV-infected mice treated with or without 1% TBBPA was measured by ELISA for each specific cytokine. Data represents mean values of 5–6 mice. Numbers in parentheses indicate standard deviation. ND, not determined.

Table 4
Effects of TBBPA on subpopulations in BAL and spleen cells of RSV-infected mice.

	% of total cell populations[a]					
	BAL cells				Spleen cells	
	Day 1 pi		Day 3 pi		Day 3 pi	
Subpopulation	Control	TBBPA	Control	TBBPA	Control	TBBPA
RSV-infected						
CD11b	91.2	92.5	24.1	24.1	10.5	6.7
CD49b	23.1	30.5	25.9	23.7	ND	ND
CD4CD8	5.3	4.0	16.0	29.1	0.1	0.1
CD3CD25	2.8	0.8	2.8	2.2	ND	ND
Mock-infected						
CD11b	ND	ND	ND	ND	6.8	7.5
CD4CD8	ND	ND	23.5	19.6	ND	ND

Spleen cells were obtained from a representative mouse in each group. ND, not determined; pi, post-infection.

[a] BAL cells were collected from 6 mice in each group on day 1 or day 3 post-infection and pooled by group.

Th1 cytokines such as IFN-γ, Th2 cytokines might be suppressed reciprocally in TBBPA-treated mice with RSV infection.

To clarify the disorder in immune cell populations due to TBBPA administration, FACS analysis was performed on BAL cells (Table 4). Initially, it was speculated that macrophages and/or dendritic cells were affected in TBBPA-treated mice, because they mainly work in the early phase of RSV infection [19] and produce IL-6 and TNF-α (Table 3). However, the percentages of CD11b+ cells did not differ in control and TBBPA-treated mice. The numbers of CD11b molecules per cell as monitored by the intensity of fluorescence did not differ in the groups either (data not shown). TBBPA might have induced a qualitative change in immune cells that worked in the early phase of RSV infection. Pullen et al. reported that activated T cells, CD3+CD25+ cells, were damaged by TBBPA in murine spleen cell cultures in vitro [12]. However, the percentages of CD3+CD25+ cell populations in BAL cells were not clearly changed by TBBPA treatment in this study. NK cells (CD49b+), which work to eliminate RSV as an early induced immune response [23], were not affected either. Only the percentages of double-positive T (CD4+CD8+) cell populations were affected by TBBPA treatment in this study. Partial inhibition of the maturation of T cells due to TBBPA may result in an increase of viral titers (Table 2). Thus, TBBPA affected not only the quality of immune cells but also the maturation of T cells in local immunity in mice.

RSV infection is an important infectious disease in the field of pediatrics because clinically severe RSV infection has been seen primarily in young children with naïve immune systems and/or genetic dispositions [3]. It was reported that RSV infection in early life was related to the risk of asthma in childhood [24,25]. Therefore, the exacerbation of RSV infection demonstrated in this study needs to be avoided in children. Moreover, developmental exposure to BFRs threatens to cause more severe disorder of the host immunity in RSV-infected mouse pups because DBDE was reported to show immunotoxicity in RSV-infected offspring mice after perinatal exposure [9], although the compound did not have that affect in this study. From the view point of the health of mothers and children, it is important to reduce contamination of the environment by TBBPA.

Acknowledgments

We thank Dr. Masaya Takeuchi (Sapporo General Pathology Laboratory, Sapporo, Japan) who stained and evaluated lung tissues. We also thank Katherine Ono for editing the manuscript. This work was supported by Health and Labour Sciences Research Grants (Research on Risk of Chemical Substances) from the Ministry of Health, Labour and Welfare of Japan and partly by Grant-in-Aid for Scientific Research (No. 20590131) and for Young Scientists (No. 20790430) from the Japan Society for the Promotion of Science.

References

[1] MacDonald NE, Hall CB, Suffin SC, Alexson C, Harris PJ, Manning JA. Respiratory syncytial viral infection in infants with congenital heart disease. N Engl J Med 1982;307:397–400.
[2] Collins PL, Chanock RM, Murphy BR. Respiratory syncytial virus. In: Knipe DM, Howley PM, editors. Fields virology. Philadelphia, Pa: Lippincott Williams&Wilkins; 2001. p. 1443–85.
[3] Holberg CJ, Wright AL, Martinez FD, Ray CG, Taussig LM, Lebowitz MD. Risk factors for respiratory syncytial virus-associated lower respiratory illnesses in the first year of life. Am J Epidemiol 1991;133:1135–51.
[4] Morales F, Calder MA, Inglis JM, Murdoch PS, Williamson J. A study of respiratory infections in the elderly to assess the role of respiratory syncytial virus. J Infect 1983;7:236–47.
[5] Sudo K, Watanabe W, Mori S, Konno K, Shigeta S, Yokota T. Mouse model of respiratory syncytial virus infection to evaluate antiviral activity in vivo. Antivir Chem Chemother 1999;10:135–9.
[6] Graham BS, Perkins MD, Wright PF, Karzon DT. Primary respiratory syncytial virus infection in mice. J Med Virol 1988;26:153–62.
[7] Wyde PR, Ambrose MW, Meyer HL, Gilbert BE. Toxicity and antiviral activity of LY253963 against respiratory syncytial and parainfluenza type 3 viruses in tissue culture and in cotton rats. Antivir Res 1990;14:237–47.
[8] Watanabe W, Shimizu T, Hino A, Kurokawa M. A new assay system for evaluation of developmental immunotoxicity of chemical compounds using respiratory syncytial virus infection to offspring mice. Environ Toxicol Pharmacol 2008;25:69–74.
[9] Watanabe W, Shimizu T, Hino A, Kurokawa M. Effects of decabrominated diphenyl ether (DBDE) on developmental immunotoxicity in offspring mice. Environ Toxicol Pharmacol 2008;26:315–9.
[10] Birnbaum LS, Staskal DF. Brominated flame retardants: cause for concern? Environ Health Perspect 2004;112:9–17.
[11] Lundgren M, Darnerud PO, Blomberg J, Friman G, Ilbäck NG. Polybrominated diphenyl ether exposure suppresses cytokines important in the defence to coxsackievirus B3 infection in mice. Toxicol Lett 2009;184:107–13.
[12] Pullen S, Boecker R, Tiegs G. The flame retardants tetrabromobisphenol A and tetrabromobisphenol A-bisallyether suppress the induction of interleukin-2 receptor alpha chain (CD25) in murine splenocytes. Toxicology 2003;184:11–22.
[13] Teshima R, Nakamura R, Nakamura R, Hachisuka A, Sawada J, Shibutani M. Effects of exposure to decabromodiphenyl ether on the development of the immune system in rats. J Health Sci 2008;54:382–9.
[14] Masutomi N, Shibutani M, Takagi H, Ueyama C, Hirose M. Dietary influence on the impact of ethinylestradiol-induced alterations in the endocrine/reproductive system with perinatal maternal exposure. Reprod Toxicol 2004;18:23–33.
[15] Kurokawa M, Tsurita M, Brown J, Fukuda Y, Shiraki K. Effect of interleukin-12 level augmented by Kakkon-to, a herbal medicine, on the early stage of influenza infection in mice. Antivir Res 2002;56:183–8.
[16] National Toxicology Program. NTP toxicology and carcinogenesis studies of decabromodiphenyl oxide (CAS No. 1163-19-5) in F344/N rats and B6C3F1 mice (feed studies). Natl Toxicol Program Tech Rep Ser 1986;309:1–242.
[17] Tada Y, Fujitani T, Yano N, Takahashi H, Yuzawa K, Ando H, et al. Effects of tetrabromobisphenol A, brominated flame retardant, in ICR mice after prenatal and postnatal exposure. Food Chem Toxicol 2006;44:1408–13.
[18] Janeway CA, Travers P, Walport M, Shlomchik MJ. Innate immunity. immunobiology: the immune system in health and disease. 5th ed. New York, NY: Garland Publishing; 2001. p. 35–91.
[19] Neuzil KM, Tang YW, Graham BS. Protective role of TNF-alpha in respiratory syncytial virus infection in vitro and in vivo. Am J Med Sci 1996;311:201–4.
[20] Canesi L, Lorusso LC, Ciacci C, Betti M, Gallo G. Effects of the brominated flame retardant tetrabromobisphenol-A (TBBPA) on cell signaling and function of *Mytilus* hemocytes: involvement of MAP kinases and protein kinase C. Aquat Toxicol 2005;75:277–87.
[21] Reistad T, Mariussen E. A commercial mixture of the brominated flame retardant pentabrominated diphenyl ether (DE-71) induces respiratory burst in human neutrophil granulocytes in vitro. Toxicol Sci 2005;87:57–65.
[22] Waris ME, Tsou C, Erdman DD, Zaki SR, Anderson LJ. Respiratory syncytial virus infection in BALB/c mice previously immunized with formalin-inactivated virus induces enhanced pulmonary inflammatory response with a predominant Th2-like cytokine pattern. J Virol 1996;70:2852–60.
[23] Hussell T, Openshaw PJ. Intracellular IFN-gamma expression in natural killer cells precedes lung CD8+ T cell recruitment during respiratory syncytial virus infection. J Gen Virol 1998;7:2593–601.
[24] Sigurs N, Gustafsson PM, Bjarnason R, Lundberg F, Schimdt S, Sigurbergsson F, et al. Severe respiratory syncytial virus bromchiolitis in infancy and asthma and allergy at age 13. Am J Respir Crit Care Med 2005;171:137–41.
[25] Stein RT, Sherrill D, Morgan WJ, Holberg CJ, Halonen M, Taussig LM, et al. Respiratory syncytial virus in early life and risk of wheeze and allergy by age 13 years. Lancet 1999;354:541–5.

Journal of Medical Virology 82:1075–1082 (2010)

Functional Disorder of Primary Immunity Responding to Respiratory Syncytial Virus Infection in Offspring Mice Exposed to a Flame Retardant, Decabrominated Diphenyl Ether, Perinatally

Wataru Watanabe,[1] Tomomi Shimizu,[2] Rie Sawamura,[2] Akane Hino,[2] Katsuhiko Konno,[3] and Masahiko Kurokawa[2]*

[1]*Department of Microbiology, School of Pharmaceutical Sciences, Kyushu University of Health and Welfare, Nobeoka, Miyazaki, Japan*
[2]*Department of Biochemistry, School of Pharmaceutical Sciences, Kyushu University of Health and Welfare, Nobeoka, Miyazaki, Japan*
[3]*Department of Clinically Veterinary Medicine, School of Pharmaceutical Sciences, Kyushu University of Health and Welfare, Nobeoka, Miyazaki, Japan*

Perinatal exposure to a representative flame retardant, decabrominated diphenyl ether (DBDE), was shown previously to increase viral titers in the lungs of respiratory syncytial virus (RSV)-infected offspring on day 5 post-infection, resulting in exacerbation of pneumonia. In this study, the significant increase of pulmonary viral titers was confirmed even on day 1 post-infection and the effect on the primary immune response to RSV infection were examined to assess a mode of DBDE action on developmental immunotoxicity. On day 1 after infection, the secretion of both TNF-α and IL-6 decreased significantly in the bronchoalveolar lavage fluid prepared from RSV-infected offspring exposed to DBDE perinatally, but IL-1β increased. However, in ex vivo lipopolysaccharide stimulation test, the productivity of TNF-α in the bronchoalveolar lavage cells, which are mainly primary immune cells responding to RSV infection, prepared from offspring mice exposed to DBDE perinatally was not lower than that in the control. The primary immune cells retained normally the ability of cytokine production after the DBDE exposure. Gene expressions of innate pattern recognition receptors (Toll-like receptor 3 and 4, melanoma differentiation-associated gene-5, and retinoic acid-inducible gene I) in lung tissues were not affected by DBDE exposure. Because the levels of TNF-α, IL-6, and IL-1β are known to be elevated in the lungs of RSV-infected mice, these irregular productions due to perinatal DBDE exposure indicate a disorder of the primary immune response to RSV infection. Thus, perinatal exposure to DBDE was suggested to cause a functional disorder of primary immunity responding to RSV infection. *J. Med. Virol. 82:1075–1082, 2010.*

KEY WORDS: decabrominated diphenyl ether; respiratory syncytial virus; TNF-α; macrophages; innate pattern recognition receptors

INTRODUCTION

Human respiratory syncytial virus (RSV), a member of the family *Paramyxoviridae*, is the most prevalent infectious agent of acute lower respiratory illness in infants and young children [MacDonald et al., 1982]. Infection and reinfection with RSV are frequent during the first few years of life and most of children are infected by age 24 months [Collins et al., 2001]. Clinically severe RSV infection has been seen primarily in young children with naïve immune systems and/or genetic predispositions [Holberg et al., 1991], patients with suppressed T-cell immunity [MacDonald et al., 1982], and the elderly [Morales et al., 1983].

Grant sponsor: Ministry of Health, Labour and Welfare of Japan (Health and Labour Sciences Research Grants [Research on Risk of Chemical Substances]; Grant sponsor: Japan Society for the Promotion of Science; Grant numbers: 20590131 and 20790430.

*Correspondence to: Masahiko Kurokawa, Department of Biochemistry, School of Pharmaceutical Sciences, Kyushu University of Health and Welfare, Yoshino 1714-1, Nobeoka, Miyazaki 882-8508, Japan. E-mail: b2mk@phoenix.ac.jp

Accepted 18 January 2010
DOI 10.1002/jmv.21770
Published online in Wiley InterScience (www.interscience.wiley.com)

Brominated flame retardants (BFRs) including polybrominated diphenyl ethers (PBDEs) are used as additive flame retardants at concentrations of 5–30% in many different polymers, resins and substrates, and common plastics, including acrylonitrile butadiene styrene and high impact polystyrene [Hedemalm et al., 1995]. As they are leached and escape from the finished polymer product, they exist ubiquitously in the environment and are suspected of being toxic to children [Fischer et al., 2006].

Decabrominated diphenyl ether (DBDE) accounts for more than 85% of PBDEs used commercially, mainly pentabrominated diphenyl ether, was reported using animal models as follows: effects on liver enzymes [Zhou et al., 2001; Lundgren et al., 2007], endocrine disruption [Ceccatelli et al., 2006; Kuriyama et al., 2007], neurotoxicity [Eriksson et al., 2002; Viberg et al., 2003], reproductive damage [McDonald, 2005; Lilienthal et al., 2006], and immunotoxicity [Fowles et al., 1994; Reistad and Mariussen, 2005; Martin et al., 2007]. It was reported that DBDE could be absorbed (>10% of the dose) orally, and the highest concentrations were found in the plasma and highly perfused tissues of rats [Mörck et al., 2003]. DBDE has also shown to be the debrominated compounds by metabolizing [Birnbaum and Staskal, 2004].

A novel assay system for evaluation of the developmental immunotoxicity of BFRs using a mouse model of RSV infection has been established and reported previously [Watanabe et al., 2008a]. Using this model, it was shown that perinatal exposure to DBDE elevated the levels of interferon-γ (IFN-γ) in the bronchoalveolar lavage fluid (BALF) of RSV-infected offspring mice with an increase of pulmonary viral titers and exacerbated pneumonia [Watanabe et al., 2008b], indicating that DBDE is a risk factor for RSV infection across the human generations. However, in cyclophosphamide-treated offspring mice, pulmonary viral titers increased, but the levels of IFN-γ decreased. Mechanisms or sites of action of cyclophosphamide, a representative immunosuppressive agent, and DBDE in RSV-infected offspring mice are different, and DBDE was suggested to affect specific site(s) of the immune system in offspring mice.

In this report, to assess a mode of action of DBDE on developmental immunotoxicity, when the significant increase of pulmonary viral titers occurs in offspring mice exposed to DBDE perinatally after RSV infection was determined and a significant increase on day 1 post-infection was observed. On day 1 after infection, to clarify effects of perinatal exposure to DBDE on the specific site(s) or the immune cells on innate immunity, the levels of several cytokines and gene expressions of innate pattern recognition receptors were compared in offspring mice exposed or unexposed to DBDE perinatally. Also, to reveal whether DBDE exposure damages the function of immune cells, the productivity of TNF-α in the bronchoalveolar lavage cells as primary immune cells responding to RSV infection were examined.

MATERIALS AND METHODS

Mice

Female (6 weeks old) and male (8 weeks old) BALB/c mice were purchased from Kyudo Animal Laboratory (Kumamoto, Japan) and housed at 25 ± 2°C. The mice were allowed free access to a conventional solid diet CRF-1 (Oriental Yeast Co., Chiba, Japan) and water and used in this experiment after 7 days acclimation. The animal experimentation guideline of the Kyushu University of Health and Welfare was followed in the animal studies.

Cells and Virus

Human epidermoid carcinoma (HEp-2) cells (American Type Culture Collection CCL-23) were purchased from Dainippon Pharmaceutical (Osaka, Japan) and maintained in Eagle's minimum essential medium supplemented with heat-inactivated 10% fetal calf serum (FCS). The A2 strain of RSV was obtained from American Type Culture Collection (Rockville, MD) and grown in HEp-2 cell cultures. Viral titers were measured using HEp-2 cells by the plaque method, and expressed as plaque-forming units per milliliter (PFU/ml) [Watanabe et al., 2008a].

Reagent

DBDE (purity: ≥98.0%) was purchased from Wako Pure Chemicals (Osaka, Japan) and mixed into a soy-free powder diet, based on the formulation of the NIH-07 open-formula rodent diet [Masutomi et al., 2004], produced by Oriental Yeast Co. (Chiba, Japan).

Perinatal Exposure to DBDE

Perinatal exposure to DBDE was performed as described in the previous report [Watanabe et al., 2008b]. Briefly, 7-week-old female mice and 9-week-old male mice were paired and fed the CRF-1 diet for 3 days. At 3 days after conception, the CRF-1 diet was replaced with a soy-free diet to avoid the estrogen-like effect of soybeans. The female mice were divided randomly into three groups for DBDE exposure at 0, 1,000, or 10,000 ppm. These mice were exposed to DBDE mixed with the soy-free diet from 10 days after conception to weaning on postnatal day 21. After weaning, offspring mice were fed the CRF-1 diet. Finally, on postnatal day 28, offspring mice in each group were used for the following RSV infection test. Throughout the experiments, both chows and drinking water were given ad libitum.

RSV Infection

A RSV infection test was performed according to the previous report [Watanabe et al., 2008b]. Briefly, 4-week-old offspring mice (control: 12 pups, DBDE exposure at 1,000 ppm: 14 pups, and 10,000 ppm: 12 pups) were infected intranasally with 5×10^6 PFU of the A2 strain of RSV under anesthesia in experiment 1

TABLE I. Effects of Perinatal Exposure to DBDE on Pulmonary Viral Titers 1 or 5 Days After RSV Infection in Offspring Mice

Group/DBDE exposure (ppm)	Pulmonary viral titers (PFU/ml)[a]			
	Experiment 1		Experiment 2	Experiment 3
	Day 1 pi	Day 5 pi	Day 1 pi	Day 1 pi
Control	1,723 ± 220 (6)	12,778 ± 3,202 (6)	11 ± 10 (3)	13 ± 5 (7)
1,000	1,879 ± 195 (7)	12,917 ± 4,853 (6)	ND	ND
10,000	2,350 ± 343* (6)	17,889 ± 6,313* (6)	272 ± 134 (3)	142 ± 112* (8)

ND, not done; pi, post-infection.
Offspring mice were infected intranasally with 5×10^6 PFU of RSV in experiment 1, and with 5×10^5 PFU in experiments 2 and 3.
[a]Values represent mean ± standard deviation. Numbers in parenthesis indicate numbers of mice used in each group.
*Statistically different from control at $P < 0.05$ (Student's t-test).

(Table I). In experiments 2 and 3 (Table I), lower titers of RSV (5×10^5 PFU) were used also to observe the apparent net increase of virus titer. On days 1 and 5 after infection, BALF was obtained from the mice under anesthesia by instilling of 1.0 ml of cold phosphate-buffered saline (PBS) into the lungs and aspirating it from the trachea using a tracheal cannula [Kurokawa et al., 2002]. Following the acquisition of BALF, the lungs were removed, frozen immediately in liquid N_2, and stored at −80°C until virus titration. Ice-cold BALF was centrifuged at 100*g* at 4°C for 10 min. After centrifugation, the supernatant was stored at −80°C until to use. The cell pellet was suspended in 0.5 ml of cellbanker-1 (Nippon Zenyaku Kogyo Co., Ltd., Koriyama, Japan) as bronchoalveolar lavage cells, and then stored at −80°C prior to use. Cellbanker-1 is used widely for freeze preservation of mammalian tissues or cells. It was reported that the cells or tissues preserved in it retained intact functions when they were thawed by appropriate procedure [Shinohara et al., 2002; Nagano et al., 2007]. Previously, it was confirmed that the levels of TNF-α from bronchoalveolar lavage cells were almost equivalent between the isolated freshly and the preserved in the reagent. Frozen lung tissue was homogenized with cold quartz sand in a homogenizer, and viral titers in the supernatants of the homogenates were measured by a plaque assay [Watanabe et al., 2008a].

Assay of TNF-α Production From Bronchoalveolar Lavage Cells

Frozen bronchoalveolar lavage cells were thawed quickly at 37°C, and suspended subsequently in RPMI1640 medium supplemented with 10% heat-inactivated FCS, 100 units/ml of penicillin G, 100 μg/ml of streptomycin, and 50 μM of 2-mercaptoethanol (RPMI medium). The bronchoalveolar lavage cell suspension from each mouse was collected and pooled in each treatment group. The viable cells were counted under a phase contrast microscope (magnification 100×). Two hundred microliters of bronchoalveolar lavage cell suspension (2.5×10^5 cells/ml) was seeded on each well in a 96-well microtiter plate and incubated at 37°C for 24 hr in a humidified air with 5% CO_2. After incubation, the culture medium was removed by aspiration and replaced in fresh RPMI medium with or without 100 ng/ml of lipopolysaccharide (*W E. coli* O127: B8, Difco, Detroit, MI; LPS) [Kurokawa et al., 2003]. Following 24 hr further incubation, the culture supernatant was harvested from each well and the amount of TNF-α was measured by ELISA.

ELISA

IL-1β and IL-6 levels in BALF were measured using specific ELISA kits (Ready-set-go, eBioscience, Inc., San Diego, CA) for IL-1β and IL-6, respectively, according to the manufacturer's instructions. IL-12 levels in BALF were measured using a specific kit (Ready-set-go, eBioscience, Inc.) for IL-12 p70, without interference by p40 monomer or the related protein IL-23, according to the manufacturer's instructions. Amounts of TNF-α in BALF and the culture supernatant of bronchoalveolar lavage cells were measured by the TNF-α ELISA kit (Ready-set-go, eBioscience, Inc.). These products were tested and found to conform to all eBioscience, Inc. Quality control release specifications. The lower limits of detection sensitivity in the kit are IL-1β, 8 (pg/ml); IL-6, 4 (pg/ml); IL-12 p70, 15 (pg/ml); and TNF-α, 8 (pg/ml). The intra- and inter-assay coefficients of variation for these ELISA were less than 10%.

Real-Time RT-PCR

Gene expressions of innate pattern recognition receptors in the lung tissues were measured by real-time RT-PCR, and the data were evaluated by normalizing results to those of mouse β-actin. Briefly, RNA was isolated from the frozen lung tissues using trizol reagent (Invitrogen Corp., Carlsbad, CA) according to the manufacturer's instructions. The isolated RNA was transcribed into cDNA by ReverTra Ace α (Toyobo Co. Ltd, Osaka, Japan) using an oligo-dT(20) primer according to the manufacturer's instructions. The Toll-like receptor 4 cDNA was amplified and analyzed on a Roche LightCycler P2000 real-time PCR system using a LightCycler FastStart DNA Master HybProbe kit (Roche Diagnostics, Indianapolis, IN) with a mouse Toll-like receptor 4 Hybprobe primer-probe kit (Nihon Gene Research Laboratories, Inc., Sendai, Japan) according to the manufacturer's instructions. Amplification and analysis of the cDNAs of Toll-like receptor 3, melanoma

differentiation-associated gene-5, and retinoic acid-inducible gene I were performed using a Roche LightCycler FastStart DNA Master SYBR Green I kit (Roche Diagnostics) with the specific primers according to the manufacturer's instructions. Pairs of specific primers were as follows: Toll-like receptor 3, forward: 5′-GATACAGGGATTGCACCCATA-3′, reverse: 5′-TCCCCCAAAGGAGTACATTAGA-3′; melanoma differentiation-associated gene-5, forward: 5′-AACACAGATGGTGCGTGCT-3′, reverse: 5′-GCCCAGCACATTTTTATGGT-3′; retinoic acid-inducible gene I, forward: 5′-GACCCCACCTACATCCTCAG-3′, reverse: 5′-GGCCCTTGTTGTTCTTCTCA-3′. The amounts of Toll-like receptor 4 cDNA (number of copies) were determined according to the manufacture's instructions. The amounts of cDNAs of Toll-like receptor 3, melanoma differentiation-associated gene-5, and retinoic acid-inducible gene I were determined by comparing the crossing point values of the cDNA samples to those of the TA vectors harboring parts of the murine genes of Toll-like receptor 3 (nt. 148–480), melanoma differentiation-associated gene-5 (nt. 944–1213) and retinoic acid-inducible gene I (nt. 83–345), respectively. Amplification and analysis of the β-actin cDNA were performed using a Roche LightCycler FastStart DNA Master SYBR Green I kit with a pair of β-actin-specific primers (forward: 5′-TGGAATCCTGTGGCATCCATGAAAC-3′, reverse: 5′-TAAAACGCAGCTCAGTAACAGTCCG-3′) The amounts of β-actin cDNA were determined also by comparing the crossing point value of the cDNA sample to those of plasmid, a TA vector harboring part of the murine β-actin gene (nt. 728–1076).

Statistical Analysis

Comparisons of pulmonary viral titers and the levels of cytokines between the control and experimental groups were carried out using Student's *t*-test. A *P*-value of 0.05 or less was considered to be significant.

RESULTS

Effect of Perinatal Exposure to DBDE on RSV Infection in Offspring

To clarify effects of perinatal exposure to DBDE on immune system in offspring mice, dam mice were exposed to DBDE dietary up to 10,000 ppm from day 10 after gestation to weaning on postnatal day 21. Although mean body weight was suppressed approximately 10% in dam mice exposed to DBDE at 10,000 ppm, there was no significant difference in body weights of offspring mice between control and DBDE-exposed group (10.6 ± 1.2 and 10.6 ± 1.2 g, respectively). No significant differences between control and DBDE-exposed group were detected in food consumption of dams (51.8 ± 4.2 and 50.4 ± 7.7 g/week, respectively), in the numbers of litter (6.8 ± 2.4 and 7.2 ± 2.1 per dam, respectively), and in the survival rates of pups (70.4 ± 12.2 and 65.2 ± 14.3%, respectively) by postnatal day 21, either [Watanabe et al., 2008b]. No particular toxicological sign or abnormal behavior was observed in dams and offspring mice. Then, offspring mice were infected intranasally with the A2 strain of RSV at 5×10^6 PFU (Table I). No change of body weights was observed in the tested offspring mice after RSV infection. However, on day 1 post-infection, the viral titers of offspring mice treated with DBDE at 10,000 ppm were increased significantly ($P < 0.05$) compared with those of controls (experiment 1, Table I). A significant increase of the viral titers on day 5 post-infection was shown as reported previously [Watanabe et al., 2008b]. When the lower virus titer (5×10^5 PFU/mouse) was used to clarify the net increase of virus yields, pulmonary viral titers of DBDE-exposed mice perinatally were markedly higher (approximately 25-fold) than those of control mice (experiment 2, Table I). The significant increase of pulmonary viral titers by perinatal DBDE exposure was confirmed by a repeated experiment (experiment 3, Table I). These results indicated strongly that the significant increase of pulmonary viral titers in offspring mice due to perinatal exposure to DBDE had occurred even on day 1 post-infection.

Effect of Perinatal Exposure to DBDE on Primary Cytokine Production in Offspring

The findings that the viral titers were enhanced already on day 1 after infection due to perinatal DBDE exposure (Table I) suggested that DBDE affected the early immune response in RSV-infected offspring mice. Then, the amounts of major cytokines (TNF-α, IL-6, IL-1β, and IL-12) induced by RSV infection in BALF of offspring mice exposed to DBDE perinatally were compared (Table II). In mock-infected offspring mice, the levels of the cytokines in BALF were under limit of detection. TNF-α, which inhibits the progress of RSV infection both directly and indirectly [Neuzil et al., 1996], was decreased dose-dependently, and the levels at 10,000 ppm were significantly ($P < 0.05$) lower than those of the control in RSV-infected offspring. The levels of IL-6 were decreased by DBDE exposure at 10,000 ppm. In contrast to these results, IL-1β which contributes to T cell activation, was increased significantly ($P < 0.05$) at 10,000 ppm compared with the control. The levels of IL-12, one of the potent immune cytokines that activates natural killer (NK) cells, were under limit of detection in this study. Thus, perinatal exposure to DBDE suppressed production of TNF-α and IL-6 but enhanced production of IL-1β in RSV-infected offspring mice.

Effects of Perinatal Exposure to DBDE on TNF-α Production From Bronchoalveolar Lavage Cells

Bronchoalveolar lavage cells were collected from RSV-infected offspring mouse on day 1 post-infection, and pooled by treatment group, and then tested for their ability on TNF-α production in vitro. Microscopic observation showed that BALF contained mainly (91–93%) the macrophage/monocyte-like cells. There was no

TABLE II. Effects of Perinatal Exposure to DBDE on Levels of TNF-α, IL-6, IL-1β, and IL-12 in Bronchoalveolar Lavage Fluid From Mock- or RSV-Infected Offspring on Day 1 Post-Infection

Group/ DBDE exposure (ppm)	Concentration (pg/ml)[a]							
	RSV-infected				Mock-infected			
	TNF-α	IL-6	IL-1β	IL-12	TNF-α	IL-6	IL-1β	IL-12
Control	136 ± 62	268 ± 97	35 ± 9	<15	<8	<4	<8	<15
1,000	79 ± 18	177 ± 58	74 ± 47	<15	<8	<4	<8	<15
10,000	51 ± 7*	119 ± 59*	78 ± 38*	<15	<8	<4	<8	<15

[a]Data represent mean ± standard deviation of 6–7 mice.
*Statistically different from control at $P < 0.05$ (Student's t-test).

significant difference in the yields of these cells between the control and DBDE-exposed group (Table III). Bronchoalveolar lavage cells were incubated 24 hr with or without LPS (100 ng/ml). After incubation, the culture supernatant was harvested and the amounts of TNF-α were measured by ELISA (Table III). In bronchoalveolar lavage cells from RSV-infected offspring exposed to DBDE at 10,000 ppm, LPS stimulation doubled approximately the amount of TNF-α compared with the control. Thus, these results suggested that the capacity of bronchoalveolar lavage cells to produce TNF-α was not damaged due to perinatal exposure to DBDE in offspring mice.

Effect of Perinatal Exposure to DBDE on Gene Expressions of Innate Pattern Recognition Receptors in Lungs of Offspring

The levels of gene expression of innate pattern recognition receptors were measured in lung tissues of offspring on day 1 post-infection (Fig. 1). Amounts of mRNA of Toll-like receptor 3 and 4, melanoma differentiation-associated gene-5, and retinoic acid-inducible gene I were measured by real-time RT-PCR and the results were normalized to the amount of β-actin mRNA. Perinatal exposure to DBDE did not affect significantly the gene expressions of these innate pattern recognition receptors in lungs of offspring mice.

DISCUSSION

To investigate the mechanism of action of DBDE on developmental immunotoxicity, pulmonary viral titers on day 1 post-infection were measured and it was revealed that those increased significantly in RSV-infected offspring mice exposed to DBDE perinatally at 10,000 ppm (Table I). As reported previously [Watanabe et al., 2008b], both the viral titers and levels of IFN-γ in BALF were elevated significantly on day 5 post-infection after perinatal exposure to DBDE compared with those of the controls. However, in RSV-infected offspring mice treated with cyclophosphamide, a non-specific immunosuppressive agent, pulmonary viral titers increased, but the levels of IFN-γ in BALF decreased. These results suggested that immunosuppressive manner of DBDE was not non-specific. This was consisted with the report that exposure to PBDE mixture suppressed induction of the selective cytokines in coxsackievirus B3-infected mice [Lundgren et al., 2009]. To clarify the effects of perinatal exposure to DBDE on the specific site(s) or cells of the immune system, the early phase, day 1, after RSV infection was focused on.

Effects of perinatal exposure to DBDE at 1,000 or 10,000 ppm on primary cytokine productions in BALF of offspring mice were examined (Table II). It was exhibited already that perinatal exposure to DBDE at 10,000 ppm exacerbated pneumonia, such as hypertrophy and/or hyperplasia of the bronchial epithelium, in RSV-infected offspring by histopathological analysis [Watanabe et al., 2008b]. Throughout this study, perinatal exposure to DBDE at 10,000 ppm did not show any toxicological sign in offspring mice. The dosage of DBDE based on the average food consumption and body weight was calculated at approximately 3,300 mg/kg/day. The dosage sounds very high, but it has reported

TABLE III. Effects of Perinatal Exposure to DBDE on TNF-α Production From Bronchoalveolar Lavage Cells and on the Yields of the Cells on Day 1 Post-Infection in RSV-Infected Offspring Mice*

DBDE exposure (ppm)	TNF-α (pg/ml)[a]		Yields of bronchoalveolar lavage cells ($\times 10^5$)[b]
	−LPS	+LPS	
Control	<35	298.0 (265.6–330.4)	2.5 (2.2–2.7)
1,000	<35	294.3 (245.7–342.8)	3.1 (1.2–5.0)
10,000	<35	590.0 (434.6–745.4)	2.5 (2.3–2.6)

*Bronchoalveolar lavage cells were collected from control, DBDE-treated at 1,000 or 10,000 ppm offspring mice on day 1 post-infection and pooled by treatment group.
[a]Data represent mean of values of two separate experiments. Numbers in parentheses indicate the range of values.
[b]Viable cells were counted under a phase contrast microscope (magnification 100×). Data represent mean of values of two separate experiments. Numbers in parentheses indicate the range of values.